Topography and Dynamics of Associative Long-term Memory Retrieval in Humans

Patrick Khader[1], Kathrin Knoth[1], Michael Burke[1], Charan Ranganath[2], Siegfried Bien[1], and Frank Rösler[1]

Abstract

■ The present study investigated the neurophysiological processes underlying associative long-term memory retrieval of objects and spatial positions by means of a modified fan paradigm with cued recall and two neuroimaging methods (electroencephalogram [EEG] and functional magnetic resonance imaging). In an acquisition phase, either one stimulus or two stimuli became associated with a noun. During retrieval, probe stimuli comprising noun pairs were presented, and participants had to recall the respective associations and decided whether the nouns are linked to each other via a commonly associated stimulus. With this design, the quality and quantity of recalled associations was systematically varied, whereas the triggering stimuli and response requirements were held constant in all experimental conditions. Recall time proved to be directly related to the number of associations fanning out from a retrieval cue. Correspondingly, the hemodynamic response (blood oxygen level-dependent [BOLD] signal) and the amplitude of slow negative EEG potentials increased monotonically with the number of associations in both left anterior and bilateral posterior cortical areas. These effects were consistently observed with content-specific topographies for the two distinct materials. Furthermore, the multimethod approach revealed a close temporal link between response times and event-related slow potential changes on the one side and a close topographical and amplitude correspondence between slow potentials and BOLD signal changes on the other. The integrated results suggest that the neuronal dynamics of associative memory retrieval are equivalent for different types of associations, but that the structural basis is clearly content-specific. ■

INTRODUCTION

The associative structure of memory has been an important research topic in cognitive psychology (Anderson & Bower, 1973; Deese, 1965) and has resulted in elaborated models of associative memory (e.g., Masson, 1995; Anderson, 1974). In contrast, the neural correlates of how humans access associative memories, and where these memories are represented in the brain, are less well understood. The neural dynamics of associative memory have been mainly studied with single cell recordings in monkeys, and with a focus on temporal lobe structures. There, ''pair coding'' neurons were found, which changed their firing rate as a function of learning new associations (Wirth, Yanike, Smith, Brown, & Suzuki, 2003; Miyashita, Kameyama, Hasegawa, & Fukushima, 1998; Sakai & Miyashita, 1991; Miyashita, 1988). Based on these and other findings, a neurophysiological theory of associative memory was proposed (Fujimichi, Naya, & Miyashita, 2004; Naya, Yoshida, & Miyashita, 2001; Miyashita et al., 1998), assuming that limbic neurons undergo rapid modification of synaptic connectivity and provide backward signals that guide a reorganization of neocortical neural circuits. This is also a central assumption of other, broader theories about the role of the neocortex for memory storage, which postulate that distributed cortical cell assemblies establish stimulus representations by means of modified synaptic connectivities (O'Reilly & Rudy, 2001; McClelland, McNaughton, & O'Reilly, 1995; Squire & Alvarez, 1995).

In contrast to the numerous studies on the formation of associations in the brain, with a sharp focus on medial-temporal lobe structures, there are fewer studies with humans that investigate the controlled retrieval of more consolidated associations from long-term memory (LTM). These revealed a crucial role of the dorsolateral prefrontal and the posterior parietal cortex for the retrieval of word associations (Sohn et al., 2005; Sohn, Goode, Stenger, Carter, & Anderson, 2003; Wheeler & Buckner, 2003) and showed that domain-specific sensory cortices become activated during memory retrieval (Wheeler & Buckner, 2003; Nyberg et al., 2001; Nyberg, Habib, McIntosh, & Tulving, 2000; Wheeler, Petersen, & Buckner, 2000). The present study seeks to extend these findings by investigating the neocortical dynamics of associative LTM retrieval of distinct materials (i.e., spatial

[1]Philipps-University Marburg, Germany, [2]University of California at Davis

and object associations) by means of multimodal neuroimaging of the whole neocortex, using the same participants and the same experimental paradigm in a functional magnetic resonance imaging (fMRI) and a corresponding electroencephalogram (EEG) experiment. Our general aim was to monitor how and where associative LTM retrieval takes place in the brain. More specifically, we pursued three questions: (1) Is it possible to distinguish between domain-specific and domain-unspecific networks relevant for associative LTM retrieval? (2) Where are domain-specific networks located and, in particular, do these networks partially or fully overlap with sensory cortices specialized for the processing of specific stimulus features? And (3), Are the time courses of retrieval-related brain activations systematically related to retrieval effort, that is, are rise time, duration, or resolution of brain activations related to the number of associations that have to be retrieved from LTM? Although the first two questions can be answered by fMRI data alone, the third question needs a combination of spatially sensitive fMRI and temporally sensitive EEG recordings.

We investigate the neural basis of associative LTM retrieval with a fan paradigm, first introduced by Anderson (1974) to study interference processes in memory, which was substantially modified for the present purpose, that is, the investigation of controlled retrieval of distinct memory contents (Rösler, Heil, & Hennighausen, 1995; Heil, Rösler, & Hennighausen, 1994). In an acquisition phase, either one stimulus or two stimuli become associated with a noun (Figure 1A). During retrieval, probe stimuli comprising noun pairs are presented, and participants have to recall the respective associations and have to decide whether the nouns are linked to each other via a commonly associated stimulus (Figure 1B and C). At the heart of this design lies a parametric variation of the number of recalled associations, depending on the word pair's level of associative fan (Heil et al., 1994; Anderson, 1974). If both words are associated with one stimulus each, participants have to make only one comparison in order to give the correct answer. If one word is associated with one stimulus and the other word with two stimuli, then one or two comparisons are required. Lastly, if both words are associated with two stimuli, then participants have to make up to four comparisons.

By means of this paradigm, the quality and quantity of activated associations was varied systematically without changing any other aspect of the retrieval situation. Most importantly, spatial and object associations were triggered by the same type of perceptual cue (i.e., an abstract noun). Thus, neither objects nor locations were presented as a cue. Therefore, it is guaranteed that material-specific cortical activations can be genuinely related to a reactivation of stored representations rather than to processing a perceptual cue.

According to the theoretical considerations described above (O'Reilly & Rudy, 2001; McClelland et al., 1995;

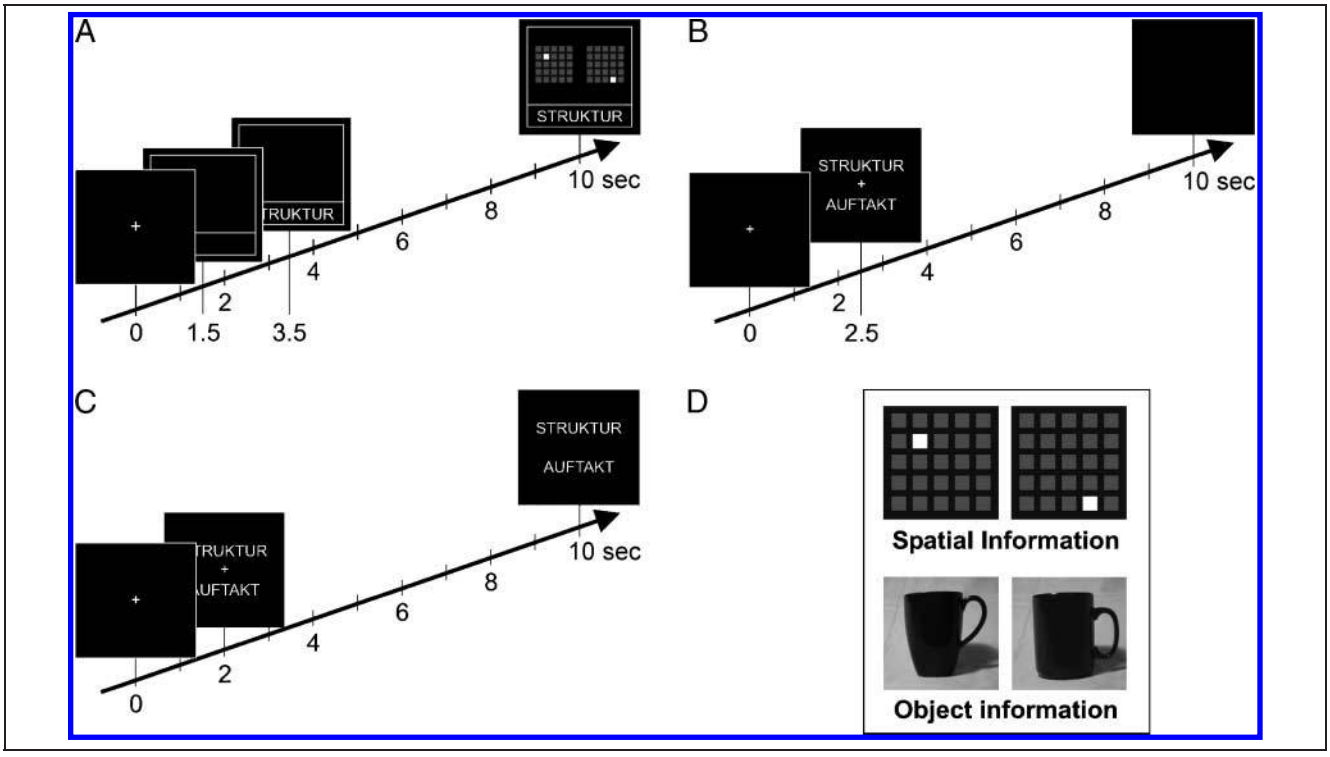

Figure 1. Stimulus sequence of acquisition (A), fMRI-recall (B), and EEG-recall (C) trials. (D) Examples of objects and positions that had to be encoded during acquisition.

Squire & Alvarez, 1995), associative memories should be distributed throughout the neocortex and bound to those areas that were active during encoding. Thus, material specificity of representations is an essential feature of these theories. A fundamental functional–anatomical dissociation during perceptual encoding and working memory tasks has been delineated for spatial versus object information (Mishkin, Ungerleider, & Macko, 1983; Ungerleider & Mishkin, 1982). Consequently, the neocortical memory model would predict a corresponding topographical dissociation when spatial and object associations are retrieved from LTM. However, in addition to the reactivation of content-specific LTM associations, additional content-unspecific processes have been proposed, which mediate the interaction between a retrieval cue and a memory trace (e.g., Buckner & Wheeler, 2001; Rugg & Wilding, 2000). Accordingly, two previous fMRI studies employed the fan effect in order to disentangle different cognitive processes during memory retrieval (Sohn et al., 2003, 2005). They found that during recognition and cued recall of word associations, the prefrontal cortex responds differently to the extent of competition during retrieval, whereas the parietal cortex seems to be responsible for problem representation that is not directly related to competition. Furthermore, these effects proved to be independent from recognition-cue modality (Sohn et al., 2005).

Based on these theories and findings, the present study seeks to disentangle content-specific and content-unspecific processes during cued recall from associative LTM, and investigates whether domain-specific sensory cortices become activated during the retrieval process. Our expectations were as follows: Brain regions that show a signal increase with increasing fan level for both objects and positions are supposed to mediate content-unspecific control processes during associative memory retrieval. In contrast, brain areas that show a fan-related signal increase for one type of material only are supposed to mediate the gradual activation of content-specific long-term associations. Moreover, if these regions show not only a content-specific fan effect, but are also more strongly activated for the one or the other stimulus type as such (i.e., independent of fan level), then these regions can be regarded as being especially important for reactivating material-specific long-term associations.

According to the assumption that the retrieval of LTM representations triggers reverberating activity in material-specific cortical cell assemblies (O'Reilly & Rudy, 2001; McClelland et al., 1995), the fan manipulation should lead to a gradual activation of these assemblies. Therefore, this process should clearly have an electrophysiological correlate in the EEG, which is an on-line measure of cortical neural activity. Previous studies of our group have repeatedly shown that the amount of cognitive effort that is necessary to perform an experimental task is proportional to the amplitude of DC-recorded event-related negative slow waves in the EEG, and that the distribution of these potentials across the scalp is strongly task-dependent (Rösler, Heil, & Röder, 1997). Negative slow waves are assumed to arise from an increase of synchronized excitatory postsynaptic potentials at neocortical pyramidal cells arranged perpendicular to the cortical surface (McCallum & Curry, 1993; Speckmann, Caspers, & Elger, 1984). Therefore, we expect that material-specific effects of associative fan should become manifest in topographically distinct patterns of negative slow waves. In more detail, we expect that with increasing retrieval effort, a systematic covariation can be observed between increases of response times (RTs) and error rates on one side and amplitudes or durations of slow waves on the other. Likewise, we expect a systematic parametric variation of the BOLD response with increasing retrieval effort. In other words, we want to use the slow waves to conceptually bridge the gap between the RTs and the fMRI data. To this end, we tested the same participants twice with the same protocol, once while the EEG was recorded and once while the BOLD signal was recorded. Both signals were integrated by estimating fMRI-restricted source localizations for the EEG generators. The idea is to monitor the temporal evolution of slow waves in those areas in which significant fMRI activation are found in order to integrate information from both signals into a coherent spatial–temporal pattern of brain activity activated during LTM retrieval.

In addition, it has to be emphasized that a close correspondence between BOLD and slow-wave response bears to the question of how EEG and fMRI signals are related as such. As will be shown, the present study provides clear evidence that BOLD and EEG signals are not only coupled in animal studies and basic sensory stimulation tasks, but also in humans while highly demanding cognitive tasks are performed. This correspondence concerns a very slow frequency range of the EEG signal that has received little attention so far in studies on EEG–fMRI couplings.

METHODS

Participants

Nineteen students of the University of Marburg were recruited. Four participants did not reach the learning criterion (see below). Therefore, the final sample comprised 4 men and 11 women for the EEG experiment (mean age 23.8 years, range 20–28). Twelve of the 15 students took part in the fMRI experiment (mean age 23.4 years, range 19–31, 8 women). fMRI data of two participants had to be discarded because of more than 30% inaccurate responses. All participants were right-handed, gave written consent to participate, and received either monetary compensation or course credit.

Material

In the acquisition phase, 54 nouns were linked to nine objects and nine spatial positions. Only highly abstract words (e.g., ''KONZEPT,'' Engl. concept) were chosen to minimize visual associations that could interfere with the acquisition of new associations. All words were randomly assigned to the stimuli for each participant. Half of the words (27) were associated with either one (18) or two (9) of the nine spatial positions, and the other half with either one or two of the nine objects, respectively. The object stimuli consisted of gray-scale photographs of nine cups (see Figure 1D for two examples) with the same background and size on each photograph. The spatial positions were nine randomly defined locations in a 5 × 5 matrix of dark gray squares that changed their luminance to light gray when relevant in a given trial. If two positions had to be associated with one word, the positions were marked in two separate matrices shown side by side in order to keep the presentation mode of the spatial positions and objects as comparable as possible.

In both the EEG and fMRI study, two words (associated with the same stimulus type) were simultaneously presented as the retrieval cue, and participants had to decide whether they were linked by a common object/position or not. Depending on the number of associations, two, three, or four stimuli had to be compared in a given trial, resulting in three levels of associative fan (1, 2, 3). Test probes were selected such that the factors of stimulus type, level of fan, and type of response were completely crossed. The EEG experiment consisted of 36 retrieval trials for each of the resulting 12 conditions (432 in total). For the fMRI experiment, another condition was introduced as a high-level baseline (''Fan0''), in which two *identical* words were presented. Thus, participants were exposed to words that had been associated with objects or positions, and were also required to respond, but there was no need for genuine memory retrieval because the correct answer (always ''yes'') could be determined using only visual comparison. The fMRI experiment consisted of 32 trials for each Fan × Stimulus type combination and the baseline condition (224 in total).

Procedure

On the first day, the associations between words and positions and words and objects were established and trained. On the second day, participants had to retrieve the learned associations from LTM while EEG was recorded. The participants retrieved the learned associations again during the fMRI experiment, which was performed 6–95 days later (depending on available scanner times; mean = 46 days).

The acquisition task consisted of an anticipation-learning paradigm (Figure 1A). Trials started with a white fixation cross, which was presented at the center of the screen for 1.5 sec. Then a white frame with an upper and a lower section appeared for 2 sec. The frame extended 7.5 cm horizontally and 6 cm vertically and the lower section was 1.2 cm in height. Two seconds later, a word appeared in the lower section (height = 0.7 cm), followed by one or two position(s) or object(s) in the upper section (stimulus onset asynchrony [SOA] = 6.5 sec). All stimuli remained on the screen until the participants started the next trial by pressing the space key of a computer keyboard. Before the start of the next trial, a blank screen was shown for 1 sec. Participants were instructed to encode the associations by forming an integrated picture of the display. All 54 trials were presented three times in randomized order. When the words were repeated, participants were told to anticipate the associated object(s) or position(s) during the interval of 6.5 sec between word onset and the presentation of the associated items. When two stimuli had to be associated with a word during acquisition, their positions were exchanged with every repeated presentation. The 162 experimental trials were presented in 27 blocks of six items, separated by an obligatory pause, which could be terminated by a button press.

During overlearning, which immediately followed the acquisition phase, participants worked with a feedback-controlled rehearsal procedure until they committed less than three errors in one complete set of 54 trials (93% correct). On each trial, the 5 × 5 matrix of squares or, alternatively, a 3 × 3 grid depicting the nine objects, was presented, and one out of the 54 words appeared below. The assignment of the objects to the nine possible locations was shuffled randomly for each object trial. The associated spatial position(s) or object(s) had to be selected by pressing one or two out of 25 black buttons arranged in a square. In case of an error, the correct position(s) or object(s) subsequently appeared on the screen. The sequence of words was varied randomly. On average, participants had to work on seven to eight sets before they met the criterion. This took about 1 to 2 hours. Participants had to work through training sets once more prior to the fMRI scan until they had reached the same overlearning criterion again. In contrast to the initial overlearning phase, the second one took about 15–30 min only.

Trials of the *fMRI* experiment (Figure 1B) had a fixed duration of 15 sec, starting with a fixation cross, followed by the word pair (SOA = 2.5 sec). The words disappeared after 7.5 sec, followed by a blank screen which lasted for 5 sec. Participants lay in the scanner in supine position with their head immobilized by a soft foam pad to minimize head movements. Participants had to indicate whether the words were linked to each other via an associated stimulus by pressing one of two buttons on an fMRI-compatible (fiber-optic) response device to indicate a ''yes'' or ''no'' response. Mapping of fingers to response categories was counterbalanced across participants. Par-

ticipants responded as fast as possible, but accuracy was stressed in the instruction. Stimuli were projected on a canvas the participants could see via two mirrors. Participants lay in the scanner for about 75 min during which four functional runs with 56 trials and the anatomical reference (after the second run) were recorded.

Trials of the *EEG* experiment (Figure 1C) started with a fixation cross, which was shown for 2 sec, followed by one word above and another one below, and remained visible until the participant pressed a response button. Eight seconds after the presentation of the word pair, the fixation cross disappeared, which marked the end of the period in which the participants should suppress eye blinks. Before the start of the next trial, a blank screen was shown for 2 sec. Participants had to press either the left or right ''Ctrl'' key of a computer keyboard to respond ''yes'' or ''no.'' After every block of six trials, a message on the screen indicated the number of errors in that block. After every 36 trials, a pause of 10 sec was enforced to enable a DC reset of the EEG.

fMRI Data Acquisition, Preprocessing, and Statistical Analysis

Anatomical and functional imaging was performed with a 1.5-T MR scanner (Signa, GE Medical Systems). Functional images with 24 transversal slices covering the whole brain were acquired with a T2-weighted EPI sequence (TR: 2.5 sec, TE: 60 msec, flip angle = 90°, FOV: 240/240 mm, matrix: 64 × 64, slice thickness: 3 mm, interslice gap: 1 mm, in-plane resolution: 3.75 × 3.75 mm) using a standard quadrature head coil. Four functional runs were recorded, consisting of 340 volumes each. Anatomical whole-head images were acquired from 124 axial slices (1.4 mm thick) using a fast-spin gradient-echo sequence (FSPGR; FOV = 240 × 180 mm, TE/TR = 4.2/11.1, 256 × 192 acquisition matrix, in-plane resolution = 0.9375 × 0.9375 mm).

Preprocessing and statistical analysis was performed with the BrainVoyagerQX software package (www.brainvoyager.com). The first four volumes of each run were discarded to allow for signal equilibration. After motion and slice scan time correction, temporal filtering (0.01 Hz high pass) and linear trend removal, the functional data were aligned with the anatomical reference from the same session, transformed into Talairach space (Talairach & Tournoux, 1988), spatially smoothed with a Gaussian kernel (full width half maximum = 6 mm), and subjected to voxelwise multisubject General Linear Models with separate predictors for each experimental condition. To account for the fact that RTs varied between 1 and 8 sec, the regressor functions were RT-adjusted (''RT-convolved HRF analysis''; see Christoff et al., 2001), that is, the length of the box-car predictor function was 1, 2, or 3 TRs, depending on whether the participants took less than 2.5 sec, 2.5 to 5 sec, or more than 5 sec to respond. All computed contrasts were Bonferroni-corrected at $p < .05$. Only voxels that were found to be part of the cortical gray matter of at least one participant (which was determined by a cortex reconstruction algorithm developed by Kriegeskorte & Göbel, 2001) were included in this correction, which resulted in t values of more than 4.8 for each contrast. Statistical maps were projected on a slightly inflated cortex reconstruction of one participant, on which concave curvature (i.e., sulci) appears in dark and convex curvature (i.e., gyri) in light gray (see Figures 3, 4, and 5). The functional data were also averaged across all voxels within regions of interest (ROIs), which were defined by selecting all contiguous active voxels in each contrast, and submitted to across-subject random effect analyses (Ranganath & D'Esposito, 2001) to test whether the mean of the individual subjects' t values was reliably different from zero. Effects were considered substantial if their significance level was below $p < .05$.

EEG Recording and Analysis

Participants sat in an electrically shielded and dimly lit experimental chamber facing a computer screen positioned slightly below eye level at a distance of 70 cm. The EEG was recorded from 61 scalp Ag/AgCl electrodes (Easycap, Falk Minow, Munich) referenced to one earlobe and re-referenced off-line to averaged earlobes. The horizontal and vertical electrooculogram was monitored with appropriate electrode pairs. The left or right mastoid (counterbalanced across participants) served as ground. Impedances were kept below 5 kΩ. Recording and digitization (sampling rate = 500 Hz) was done with two 32-channel amplifiers (SYNAMPS, NeuroScan) and the NeuroScan software Acquire. DC drift was corrected (Hennighausen, Heil, & Rösler, 1993) and eye blinks were detected by means of cross-correlations with a template and linearly interpolated. Trials with other artifacts were removed by applying threshold criteria (e.g., maximum voltage range within a trial segment should be lower than 200 μV). Trials with correct responses were baseline-adjusted to the average amplitude of a 500-msec epoch preceding the onset of the words in the retrieval phase and averaged separately for participants, electrodes, and experimental conditions. For the statistical analysis, average voltage amplitudes were computed for consecutive intervals of 50 msec from 0 to 1.5 sec after stimulus onset (event-related potential [ERP] analysis), and for intervals of 1 sec, beginning 1.5 sec after the onset of the words and ending 6 sec later (slow-wave analysis). A subset of electrodes equivalent to the 19 standard electrodes of the 10–20 system entered the statistical analysis. Effects of interest were tested with repeated-measures analyses of variance (ANOVAs) with factors electrodes, stimulus type, and level of fan for each time epoch. Error probability was corrected according to Huynh and Feldt (1976) to account for nonsphericity.

EEG Source Localization

In addition to the visual comparison of EEG and fMRI topographies, the convergence between slow waves and BOLD signals was also accessed by means of EEG source localization. The aim of these analyses was to establish a functional link between areas showing material-specific fan effects in the fMRI and the surface-recorded slow-wave topographies. It has to be stressed that our goal was not to explain the ERP topography by solving the ''inverse problem'' (i.e., to estimate generators from the EEG topography and to look for how closely these estimates covary with the BOLD signal activation pattern). Rather, we wanted to test whether the strengths of dipoles seeded in those areas that show effects of interest in the fMRI can ''explain'' the EEG signal changes, in particular, the temporal development of amplitude changes and the overall topography of slow waves.

To this purpose, the averaged difference waves of fan level (''Fan3 − Fan1'') and stimulus type (''positions − objects'') were modeled by fixed equivalent dipoles (using BESA), whose locations were derived from the centers of gravity of fMRI activation clusters that showed up in the corresponding fMRI contrasts of fan level and stimulus type at p(corrected) < .05. In the fan contrasts, some areas were found to be activated by both positions and objects. In those cases, the locations of the dipoles were derived by averaging the x, y, and z Talairach coordinates of the centers of gravity of the activation clusters for objects and positions. The dipoles' positions were completely determined by the Talairach coordinates, whereas their orientations (as well as their strengths for each time point from 0 to 7.5 sec) were fitted to explain a maximum amount of variance of the EEG signal. Prior to fitting, a 10-Hz low-pass filter (zero phase, 12 dB/oct) was applied to the data.

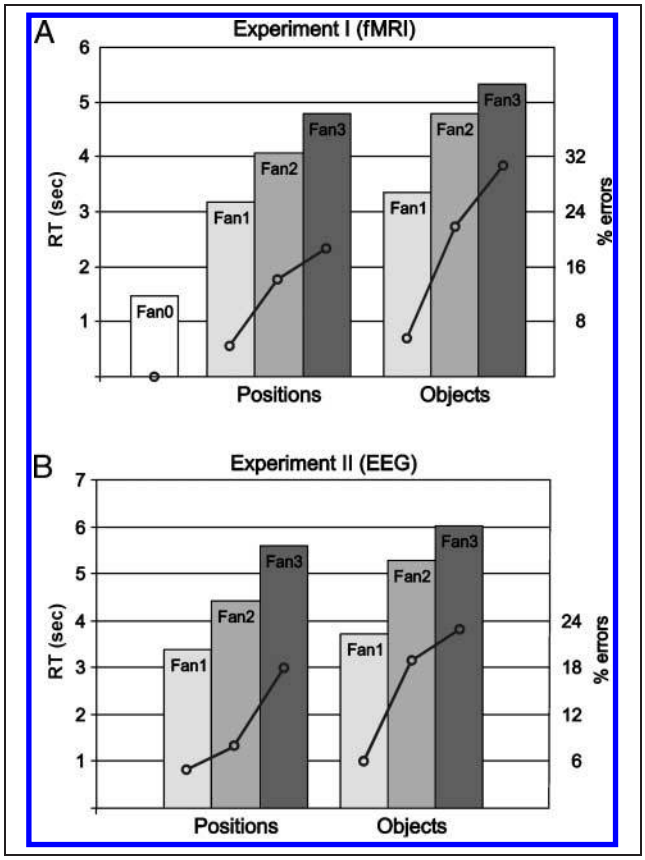

Figure 2. Mean percentage of accurate judgments (depicted as line insets) and response times [RTs] (depicted as bars) in the fMRI (A) and EEG experiment (B), separately for stimulus type and fan level. For both positions and objects in both experiments, RTs and error rates increased with increasing fan.

RESULTS

Behavioral Data

Mean RT and error rates of both experiments were submitted to ANOVAs with factors stimulus type (objects/positions) and level of associative fan (1/2/3). RTs from incorrect responses and outliers (RT < 300 msec and RT > 2.5 *SD* for each participant and experimental condition) were discarded. RTs and error rates of the *fMRI* experiment are presented in Figure 2A. Obviously, the level of fan had a substantial effect on both measures. Overall accuracy varied between 75% and 94% over participants (mean = 84.0%, *SD* = 6.2%). The ANOVA revealed significant main effects of fan level [$F(2,18) = 28.96$, $p < .0001$, $\varepsilon(H - F) = .840$], and stimulus type [$F(1,9) = 6.56$, $p = .0306$]. t Tests showed that accuracy decreased significantly with increasing fan and that, generally, more errors were made during the recall of objects. Two additional t tests revealed that in condition ''Fan0,'' participants were significantly more accurate than in both ''Fan1'' conditions. RTs showed main effects of fan level [$F(2,18) = 27.50$, $p < .0001$, $\varepsilon(H - F) = .976$] and stimulus type [$F(1,9) = 57.64$, $p < .0102$], as well as an interaction [$F(2,18) = 7.30$, $p = .0123$, $\varepsilon(H - F) = .707$]. t Tests showed that RTs increased significantly with increasing fan for both positions and objects, and that recalling objects took longer only at the intermediate fan level.

RTs and error rates of the *EEG* experiment are shown in Figure 2B. The number of correct responses varied between 77% and 96% over participants (mean = 87%, *SD* = 6.3%), and the ANOVA revealed main effects of fan level [$F(2,28) = 23.53$, $p < .0001$, $\varepsilon(H - F) = .742$] and stimulus type [$F(1,14) = 10.85$, $p = .0053$], as well as a significant interaction [$F(2,28) = 5.67$, $p = .0129$, $\varepsilon(H - F) = .843$]. One-way stimulus-specific ANOVAs with factor fan proved that both objects and positions showed a significant fan effect. However, the difference between the lowest and the intermediate fan level was significant only for objects, whereas the intermediate and highest levels differed significantly only for positions. Furthermore, recalling objects produced significantly more errors only at the intermediate level. The RT-ANOVA revealed again main effects of fan

level [$F(2,28) = 120.62, p < .0001, \varepsilon(H - F) = .870$] and stimulus type [$F(1,14) = 19.71, p = .0006$], as well as a significant interaction [$F(2,28) = 3.96, p = .0373, \varepsilon(H - F) = .871$]. t Tests revealed that RTs increased significantly with increasing fan for both types of stimuli, and that recalling objects took longer at all fan levels. Furthermore, the difference between the lowest and intermediate levels proved to be higher when recalling objects.

To summarize, both RTs and error rates increased significantly with increasing fan for both objects and positions in both the EEG and fMRI experiments. Furthermore, they were generally higher for objects at all fan levels (EEG-RTs, EEG-errors, and fMRI-errors), or at the intermediate level only (fMRI-RTs).

Event-related Hemodynamic Signal Changes

First, we determined areas that responded parametrically to the number of to-be-retrieved associations by computing linear fan contrasts (Fan0 < Fan1 < Fan2 < Fan3). Figure 3 shows a superposition map of these contrasts for positions (orange to yellow) and objects (blue to green). Obviously, many areas exhibited a monotonic increase of the BOLD signal with increasing fan, which is illustrated in Figure 3 by time plots of event-related BOLD signals, averaged to cue onset. Areas that strongly responded to both materials consisted of the left and right superior and left inferior parietal lobe, as well as the left middle and inferior frontal gyrus. In addition, when spatial associations had to be retrieved, a fan-related BOLD response was also seen in the left and right parastriate cortex (BA 18, cuneus), the left and right superior occipital gyrus, as well as the right inferior parietal lobe and the left and right precentral cortex (see Table 1). The left frontal cortex activity was more extended for objects, whereas the parietal activity was more extended for positions. All activations were substantiated by subsequent ROI random effect analyses [except of the right superior parietal lobe for objects ($p = .083$) and the right inferior parietal lobe for positions ($p = .088$), which reached marginal significance only].

With a second analysis, we were interested in areas that are generally more active during the retrieval of spatial or object associations, independent of the number of

Table 1. Location, Peak t Value, and Number of Significantly Activated Voxels of Brain Areas that Show a Linear Increase in Activation with Increasing Level of Associative Fan (p corrected < .05)

Region	*BA*	*x*	*y*	*z*	*t*	*Voxels*
Positions						
L middle/inferior frontal gyrus	9/46	−47	21	30	9.19	4401
L middle frontal gyrus	6/9	−44	5	35	10.19	5187
L precentral gyrus	6	−30	−4	53	11.41	4442
R precentral gyrus	6	25	−5	52	10.55	3355
L superior parietal lobe	7	−12	−68	46	15.73	10001
R superior parietal lobe	7	14	−69	42	13.90	11212
L inferior parietal lobe	7/40	−35	−47	41	10.14	5936
R inferior parietal lobe	7/40	32	−45	40	7.81	883
L superior occipital gyrus	19	−27	−70	28	10.02	4007
R superior occipital gyrus	19	24	−70	33	12.56	5361
L occipital gyrus/cuneus	18	−18	−60	17	9.39	3983
R occipital gyrus/cuneus	18	14	−57	14	10.34	3821
Objects						
L middle/inferior frontal gyrus	9/44/45	−45	19	30	2.83	7964
L middle frontal gyrus	9	−44	3	37	11.12	5459
L middle frontal/precentral gyrus	6	−36	1	54	7.59	1359
R superior parietal lobe	7	27	−61	37	7.65	1547
L superior parietal lobe	7	−28	−65	36	10.59	3541
L inferior parietal lobe	7/40	−29	−55	37	10.52	3213

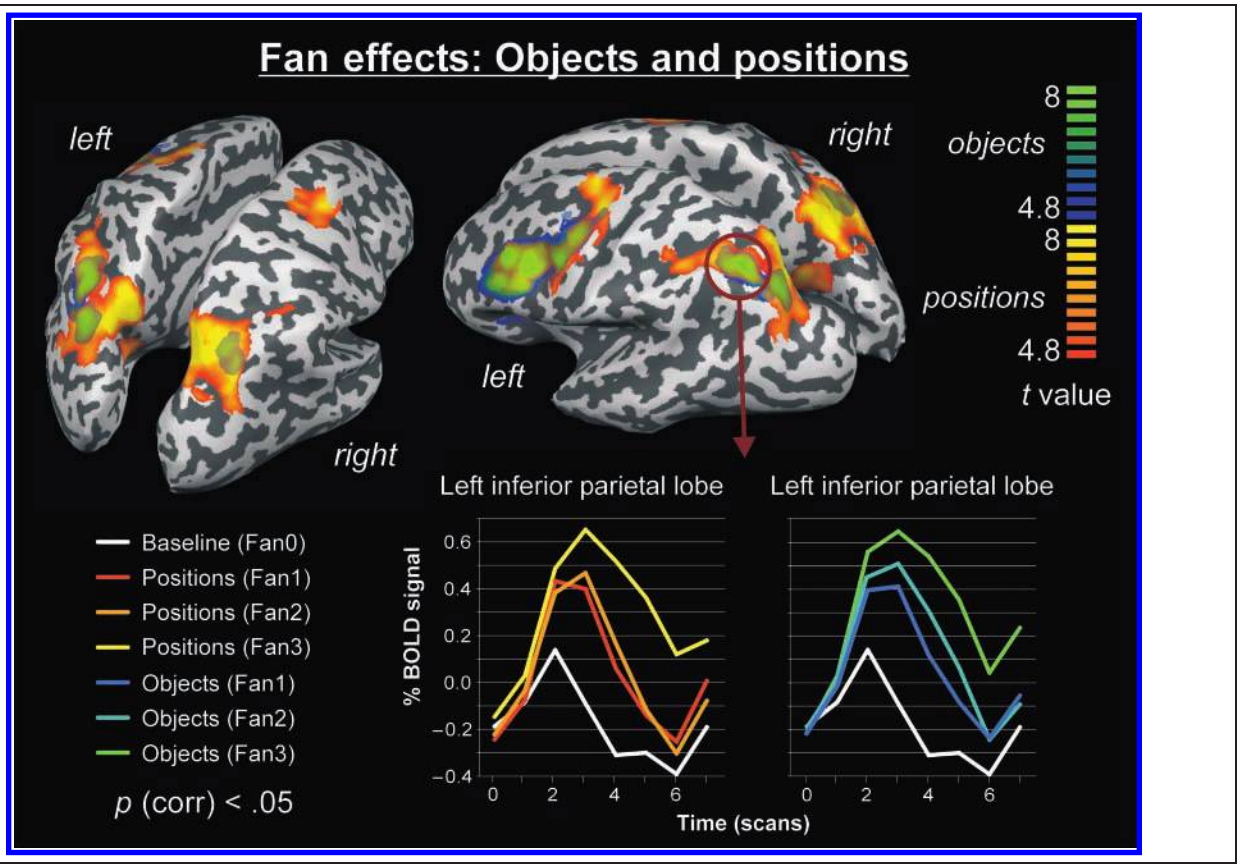

Figure 3. Brain areas showing a monotonic activation increase with increasing associative fan. Superimposed are the fMRI fan contrasts (3 > 2 > 1 > 0) for recalling objects (blue–green) and positions (red–yellow). Activations are projected on the partially inflated cortex reconstruction of one participant shown in three different orientations (left, inferior, and right view). Below are illustrative plots of event-related BOLD signals (averaged to cue onset) from a brain region that shows a pronounced effect of associative fan in the BOLD signal. The units on the time axis correspond to scans (i.e., 2.5 sec).

associations. Therefore, a contrast was computed for recalling spatial versus object associations, independent of fan level (Figure 4 and Table 2). For positions, all areas that exhibited a fan-related increase of activity also showed more activation compared to objects in this general contrast. Additional activations were found in the left and right parahippocampal, as well as in the right middle temporal cortex. In contrast, recalling object associations activated only the left middle/inferior frontal gyrus (BA 45/46) and the left middle temporal gyrus. All

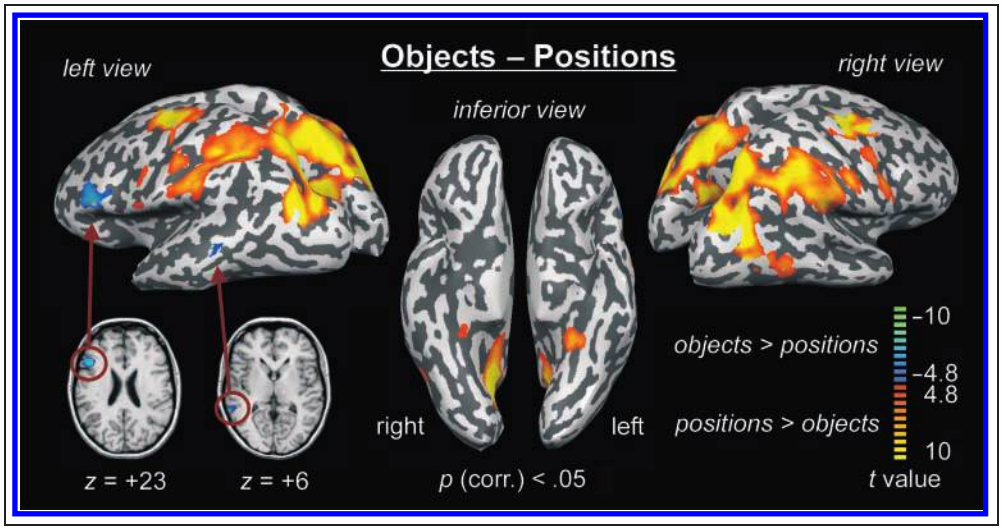

Figure 4. fMRI contrast of recalling positions (red–yellow) versus objects (blue–green), independent of the number of to-be-retrieved associations.

Table 2. Location (Region, Brodmann's Area, and Center of Gravity in Talairach Coordinates), Peak *t* Value, and Number of Activated Voxels of Brain Areas Differentiating between the Retrieval of Spatial and Object Associations (p corrected $< .05$)

Region	*BA*	*x*	*y*	*z*	*t*	*Voxels*
Positions > Objects						
L precentral gyrus	6	−26	−8	53	15.26	7254
R precentral gyrus	6	24	−7	53	15.82	5794
L precentral gyrus	4/6	−57	−1	15	5.50	281
L precentral gyrus	4/6	−58	−3	34	6.52	862
R precentral gyrus	4/6	50	0	38	8.01	3804
L superior parietal lobe	7	−15	−60	49	20.35	22092
R superior parietal lobe	7	8	−63	46	21.93	22755
L inferior parietal lobe	40/7	−36	−41	48	10.91	9264
R inferior parietal lobe	40/7	38	−43	44	13.45	15546
L inferior parietal lobe	40	−53	−24	38	9.03	6890
R inferior parietal lobe	40	53	−25	39	9.57	4971
L superior/middle occipital gyrus	19	−28	−73	23	15.13	5894
R superior/middle occipital gyrus	19	26	−72	24	18.05	7779
L parastriate cortex (cuneus)	18/31	−18	−60	17	13.12	6843
R parastriate cortex (cuneus)	18/31	11	−58	15	17.87	9143
R middle temporal gyrus	37	43	−58	3	7.10	1256
L parahippocampal gyrus	35	−29	−38	−7	8.64	1255
R parahippocampal gyrus	35	29	−35	−8	5.64	277
Objects > Positions						
L middle/inferior frontal gyrus	45/46	−50	24	20	7.79	2412
L middle temporal gyrus	21/22	−59	−40	8	5.60	479

activations for positions and objects were substantiated by subsequent ROI random effect analyses.

Finally, we determined those brain regions that exhibit stronger activity for one type of content *and* a pronounced fan effect. These areas should be most involved in LTM retrieval of spatial or object associations. For this purpose, we performed conjunction analyses of the fan and the general contrast for both positions and objects (Figure 5). In these analyses, the left middle/inferior prefrontal cortex was activated for objects, but not for positions, whereas the inferior and superior parietal lobe and precentral gyrus were activated for positions, but not for objects. This is illustrated in Figure 5, showing a fan effect and generally stronger activity for positions in the right superior parietal lobe, and a fan effect and generally stronger activity for objects in the left middle/inferior prefrontal cortex.

To further test the hypothesis of a content-specific activation of the left prefrontal and left and right superior parietal lobes, we performed ROI analyses on these areas found active in the conjunction analyses by contrasting the left middle/inferior frontal gyrus (Talairach coordinates [*x*/*y*/*z*]: −50/24/23, 1618 voxels), with the right and left superior parietal lobes (left: 12/−69/46, 2543 voxels; right: −12/70/43, 2135 voxels). Two ANOVAs, with factors ROI, stimulus type, and fan level, were computed for the first seven volumes after the presentation of the retrieval cues (i.e., from 0 to 17.5 sec). The dependent variable consisted of the percent of BOLD-signal change of these volumes relative to a prestimulus baseline of two volumes length. The first ANOVA compared the left middle/inferior frontal gyrus with the *right* superior parietal lobe and revealed an interaction of Stimulus type × ROI between 5 and 17.5 sec (all Fs > 15, $p < .01$) and of Stimulus type × Fan level × ROI between 7.5 and 12.5 sec [7.5–10 sec: $F(2,18) = 4.32$, $p = .0293$, $\varepsilon(H - F) = 1$; 10–12.5 sec: $F(2,18) = 3.72$, $p = .0610$, $\varepsilon(H - F) = .761$]. Subsequent ANOVAs with factor fan level indicated a significant (i.e., $p < .05$) fan effect for objects exclusively in the left

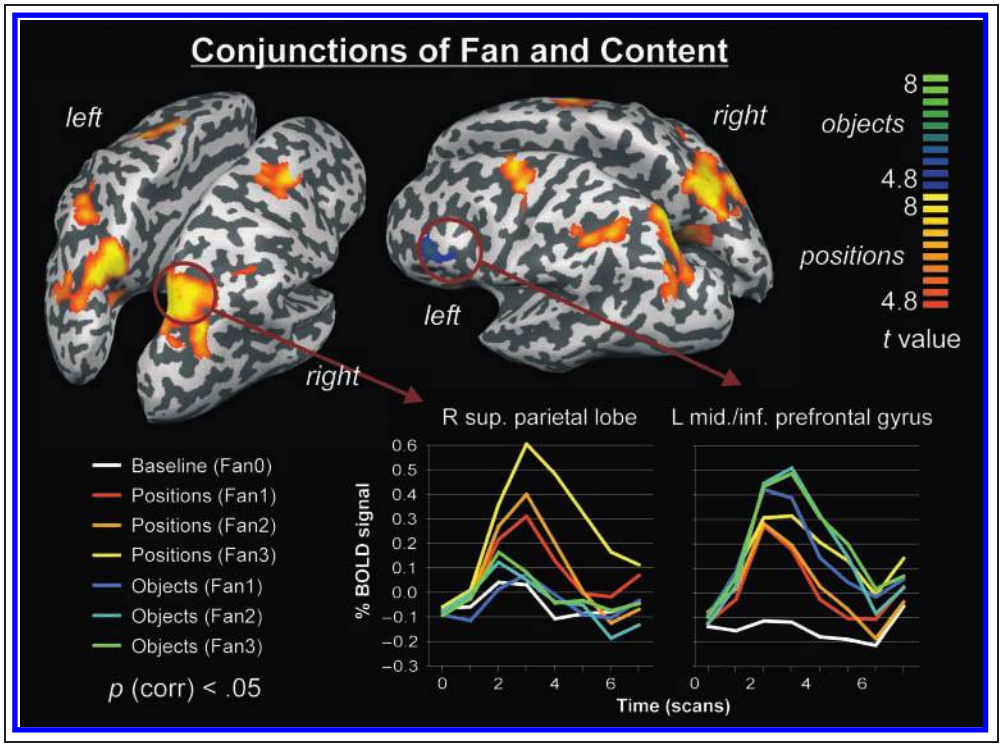

Figure 5. Brain areas showing a linear increase in activation with increasing associative fan and a general preference for either positions or objects. Superimposed are the results of the conjunction analyses of the "material type" and the "level of fan" contrasts, showing areas which responded stronger to objects *and* also revealed a fan effect for objects (blue–green), as well as areas that responded stronger to positions *and* also revealed a fan effect for positions (red–yellow). The plots below illustrate event-related BOLD signals (averaged to cue onset) from the right inferior parietal lobe showing a fan effect and stronger activity for position than object recall, as well as from the left middle/inferior prefrontal gyrus showing a fan effect and stronger activity for object than position recall.

frontal ROI between 7.5 and 10 sec, and a significant fan effect for positions between 7.5 and 12.5 sec only in the right parietal ROI. Furthermore, the BOLD signal for positions was significantly higher than for objects in the right superior parietal cortex, whereas the opposite held for the left middle/inferior frontal gyrus.

The second ANOVA compared the left middle/inferior frontal gyrus with the *left* superior parietal lobe and also revealed an interaction of Stimulus type × ROI between 5 and 17.5 sec (all Fs > 18.5, $p < .001$), with generally more activity for positions in the left superior parietal lobe and more activity for objects in the left middle/inferior frontal gyrus, but no interaction of Stimulus type × Fan level × ROI.

Event-related Potentials

As can be seen in Figure 6A, the increasing number of to-be-reactivated associations became manifest in a pronounced monotonic increase of negative slow-wave amplitude with increasing fan level. Figure 6B shows that the topography of this effect is centered over parietal electrodes for positions, but is more evenly distributed toward left frontal sites for objects. Accordingly, we found a significant interaction of Fan level × Electrodes between 2.5 and 5.5 sec (all Fs > 2, $p < .05$) in the spatial condition, and between 2.5 and 7.5 sec in the object condition (all Fs > 2, $p < .05$). To capture the maximum effect for positions and objects, electrode-specific ANOVAs with factor fan level were run for the significant time epochs. In order to reduce the probability of type I errors, only those electrodes regarded as significant that showed up in at least two adjacent time windows with $p < .05$ were included. The ANOVAs revealed a significant fan effect at parietal electrodes P4 and Pz between 3.5 and 5.5 sec in the spatial condition. In the object condition, the fan effect was also significant at parietal electrodes (P3, P4, Pz), but later, namely, from 4.5 to 6.5 sec. In addition, the object fan effect was significant at left to central frontal (F3, Fz, C3, Cz) electrodes between 4.5 and 7.5 sec, as well as at occipital (O1, O2) electrodes between 2.5 and 4.5 sec, and at T6 between 2.5 and 6.5 sec. The topographical difference between the fan effect for objects and positions can also be seen in Figure 6B, showing the topographic maps of the difference "Fan3 − Fan1" for objects and positions during the significant time epochs.

Figure 7 shows that the ERPs during the recall of spatial and object associations, independent of fan level, exhibit material-specific topographies that correspond with the material-specific topographies of the fan effects. This is supported by a highly significant interaction of Stimulus type × Electrodes from 1.5 to 7.5 sec (all Fs > 6.5, $p < .0001$). t Tests revealed that recalling positions elicited more negative potentials than recalling objects at parietal and occipital electrodes (P3, P4, Pz, O1, and O2), whereas the opposite was found at (predominantly left) frontal (F3, F4, F7, F8, Fz, Fp1, Fp2) and anterior temporal electrodes (T3 and T4).

Integration of Methods

Based on the finding that both fMRI and EEG signals showed significant increases with increasing fan level for

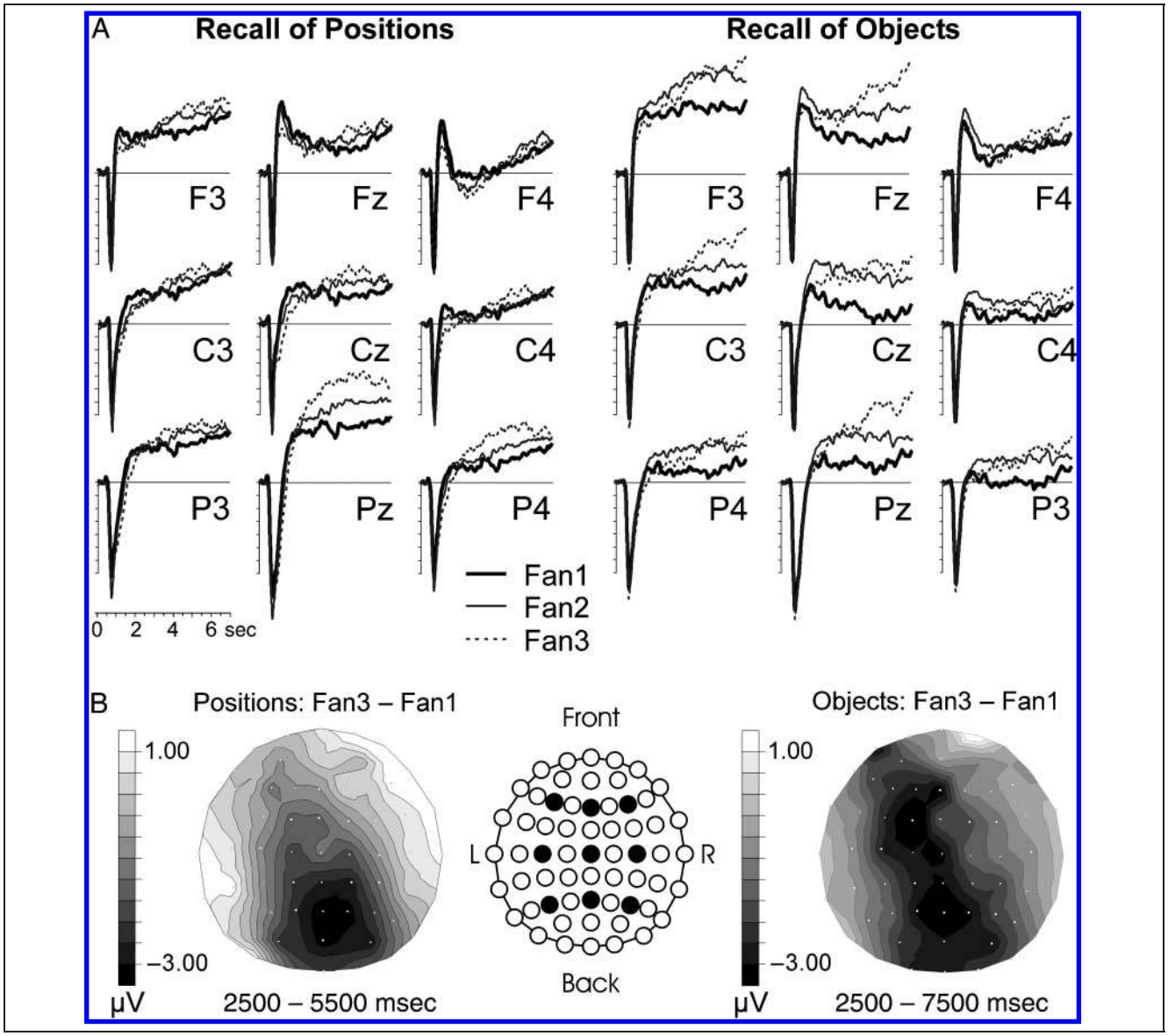

Figure 6. ERPs during retrieval of spatial and object associations for different levels of fan. (A) ERPs showing that an increasing level of fan was mirrored by a corresponding increase of negative slow-wave amplitude. (B) Topographic difference maps of "Fan3 − Fan1" between 2500 and 7500 msec after onset of the retrieval cue for objects, and between 2500 and 5500 msec for positions, as well as a scheme of the locations of all 63 scalp electrodes. The filled circles indicate the electrodes for which ERPs are depicted in A. The fan manipulation provided a systematic amplitude increase for positions at parietal electrodes, whereas this effect was more broadly distributed toward central and left frontal electrodes when object associations had to be retrieved.

both objects and positions, we first defined a model for the fan effects (i.e., the difference potentials of "Fan3 − Fan1"), which consisted of eight dipoles that correspond to all activated areas of the fan contrasts for positions and objects [i.e., the left middle/inferior frontal gyrus (−46/20/30), left middle frontal gyrus (−44/4/36), bilateral superior parietal lobes (left: −20/−66/41, right: 20/−65/39), bilateral inferior parietal lobes (−32/−51/39, 32/−45/40), and bilateral precentral cortex (−30/−4/53, 25/−5/52)]. This model was then applied to the individual fan effects for objects and positions to investigate whether the relative dipole strengths would reflect the relative amount of fMRI activation in these brain regions (i.e., whether the left inferior and middle frontal dipoles would be stronger for objects, and the opposite should hold for the parietal and precentral dipoles). The model was found to fit the fan effect for positions generally better (explained variance = 91.46%) than the fan effect for objects (78.55%). As shown in Figure 8A, the obtained source waveforms behaved as expected, that is, both parietal and the right precentral dipoles were stronger for positions, whereas the left frontal dipoles were stronger for objects. The only exception was the left precentral dipole, which was more active for objects.

Based on this close correspondence, the dynamics of the activated areas found in the fMRI analysis can be

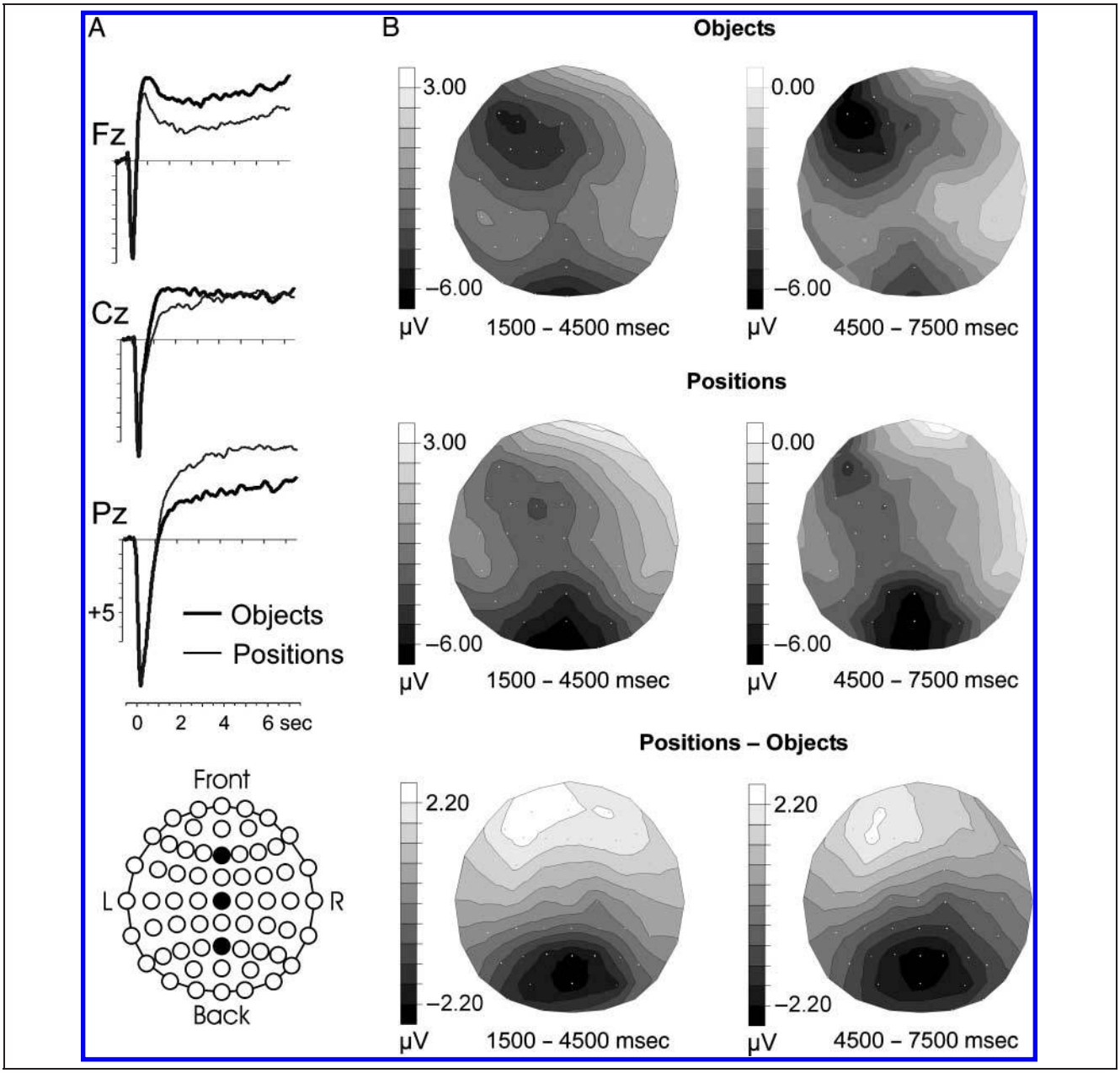

Figure 7. ERPs during retrieval of objects and positions, averaged over all levels of fan. (A) ERPs showing that objects elicited more negative potentials at frontal electrode Fz, whereas positions elicited more negative potentials over posterior electrode Pz. Below the locations of all 63 scalp electrodes are shown. The filled circles indicate the midline electrodes Fz, Cz, and Pz (from front to back). (B) Maps of the ERPs for positions and objects between 1500 and 7500 msec after onset of the retrieval cue, as well as the corresponding difference maps of "positions − objects."

Figure 8. Locations and ERP dipole source waveforms of two fMRI-seeded dipole models. (A) Model for the EEG difference waves of "Fan3 − Fan1" for positions and objects, whose dipole locations were derived from the corresponding fMRI fan contrasts. In the partial 3-D model, the pin-roots mark the dipole positions in *x*- and *y*-coordinates on the horizontal plane and the pinheads show the height of the dipole position above to the horizontal plane (*z*-coordinate). Dipole orientations were fitted to best explain the EEG variance of the fan difference potentials for positions and objects. The source waveforms show that the left frontal dipoles are stronger when retrieving objects compared to positions, whereas the opposite holds for the parietal and right precentral dipoles. (B) Model for the difference between positions and objects, whose dipole locations were derived from the corresponding fMRI contrast. Dipole orientations were fitted to optimally explain the EEG variance of the raw ERPs of positions and objects. The source waveforms show that the left frontal dipole is stronger when recalling objects compared to positions, whereas the opposite holds for the precentral and parietal dipoles.

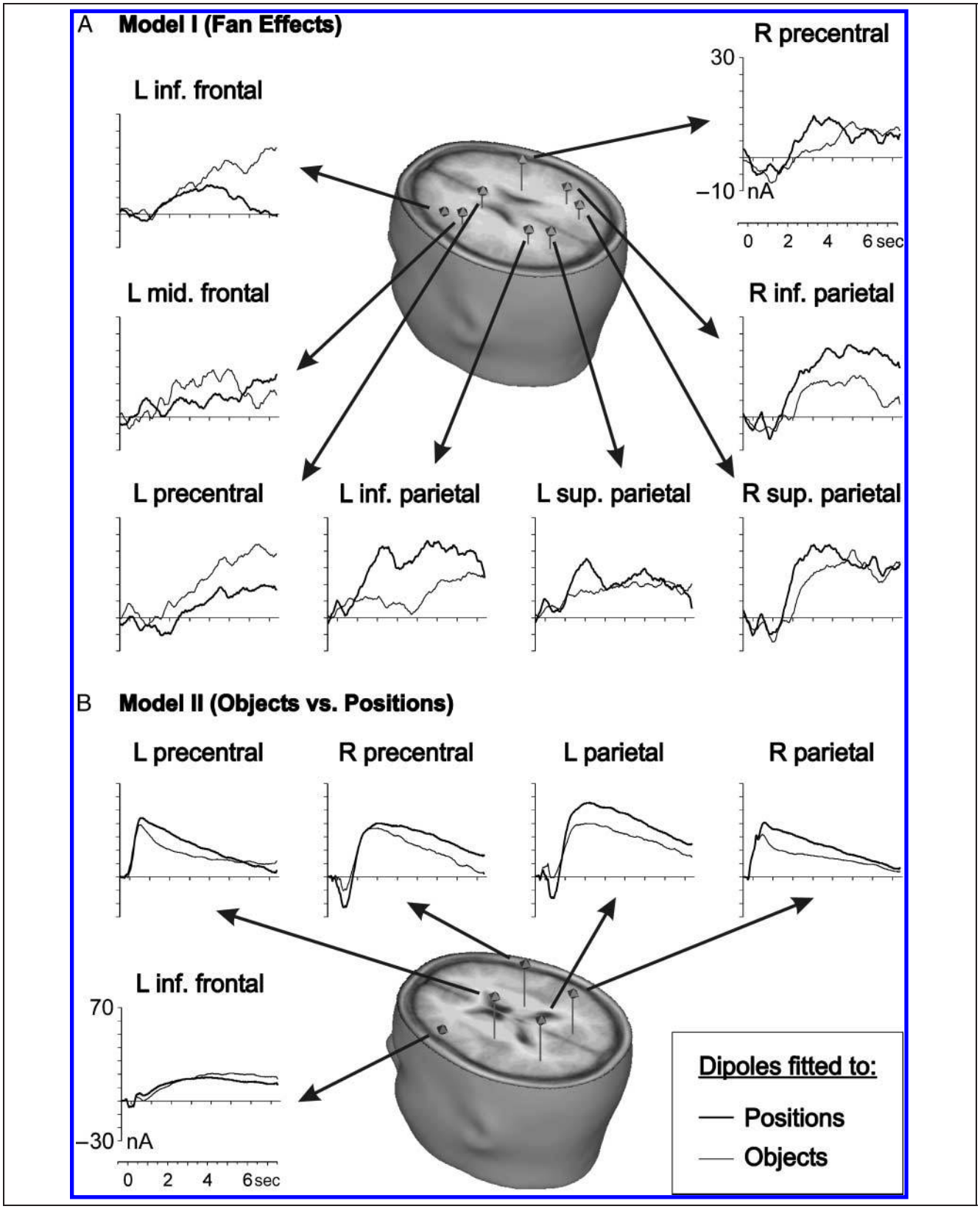
A
Model I (Fan Effects)
R precentral
30
–10
nA
0 2 4 6 sec
L inf. frontal
L mid. frontal
R inf. parietal
L precentral
L inf. parietal
L sup. parietal
R sup. parietal
B
Model II (Objects vs. Positions)
L precentral
R precentral
L parietal
R parietal
L inf. frontal
70
–30
nA
0 2 4 6 sec
Dipoles fitted to:
Positions
Objects

inferred from the temporal characteristics of the corresponding source waveforms. The source waveforms in Figure 8A show that for the dipoles with a stronger object than position fan effect, the object fan effect is initially small but increases later on. In contrast, for the dipoles with a stronger spatial than object fan effect, the position fan effect reaches its maximum earlier and remains constant or decreases toward the end of the modeled period. This finding corresponds nicely with the original ERP fan effects (see Figure 6A and ERP results), where the fan effect for objects at left central and frontal electrodes was significant during later time epochs compared to the fan effect for positions at parietal electrodes.

In a next step, we also tried to explain the general difference between materials (i.e., the variance of the difference ''objects − positions''). Five dipoles, which were seeded according to the contrast of objects versus positions in the left and right precentral cortex (−26/−8/53, 24/−7/53), in the left and right parietal lobes (−25/−50/48, 23/−53/45), and in the left middle/inferior frontal gyrus (−50/24/20), explained nearly the total variance of the EEG topography (residual variance = 3.75%). This model was applied to the raw topographies of objects and positions to investigate whether the left frontal dipole is stronger for objects and the precentral and parietal dipoles are stronger for positions. As can be seen in Figure 8B, all obtained source waveforms exactly behaved as expected, that is, the parietal and precentral dipoles were stronger for positions, whereas the left frontal dipole was stronger for objects. The source waveforms in Figure 8A also show, in close correspondence with the temporal activation differences between frontal and parietal areas found with the fan effects, that the frontal difference between objects and positions is initially weak, but becomes increasingly stronger, whereas the difference in more posterior regions reaches its maximum earlier and remains constant, or decreases, toward the end of the modeled period.

With the BESA analysis, the strengths of dipoles were estimated at ''seeded'' locations where the BOLD signal had shown a maximum response. This procedure tested whether the strengths of estimated slow-wave sources correspond to the BOLD signal strengths and, as we have seen, revealed a high correspondence, suggesting that the cortically recorded electrical changes are indeed most likely generated within the predefined cortex locations. A less restrictive approach is provided if locations and strengths of EEG activation sources were estimated without any fMRI-derived constraints and if these unconstrained source estimates corresponded with the BOLD response patterns. We used LORETA-KEY software (KEY Institute for Brain-Mind Research, University Hospital of Psychiatry, Zurich, Switzerland) and estimated such unconstrained sources for the overall material-specific topographies (independent of fan level) and for the fan effects (difference maps of Fan3 − Fan1) for objects and positions. To reduce the amount of data, ERP grand averages were downsampled to 50 Hz, and a 10-Hz low-pass filter was applied prior to source modeling. LORETA images were computed for those time epochs in which significant differences be-

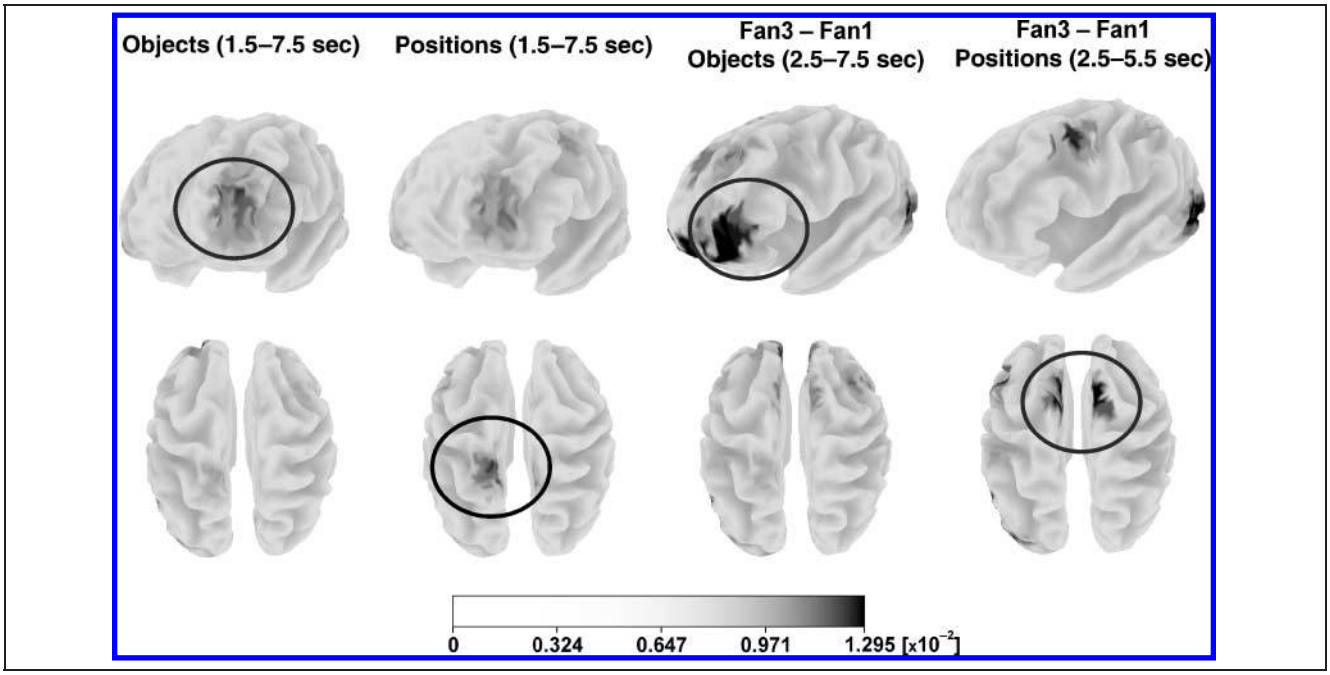

Figure 9. Distributed source-density maps (LORETA) for the overall material-specific topographies (independent of fan level) and for the fan effects (difference maps ''Fan3 − Fan1'') for objects and positions, computed for those time epochs in which significant ERP differences between objects and positions were found in the statistical analysis of the ERP data.

tween objects and positions had been found in the ERP data (see Figures 6 and 7). Figure 9 summarizes the LORETA results, which again show differences between the two materials and the fan effects. Consistent with the BESA analysis, the retrieval of objects produced slightly higher source strengths in the left frontal cortex, whereas the retrieval of positions produced higher source strengths in the parietal cortex. A more pronounced difference between objects and positions in the left frontal cortex is revealed by the different source models of the fan effects, showing that the fan effect for objects is associated with stronger sources in the left frontal cortex. In contrast, the fan effect for positions produced slightly higher source strengths in the precentral cortex. This is also consistent with the fMRI analysis, where the fan contrast for positions was much stronger in the left and right precentral cortex. According to the BOLD and the slow-wave topographies, we had expected this LORETA effect to be located more posterior in the parietal cortex. Nevertheless, LORETA approximated the distribution of neural activations obtained with the fMRI analysis also quite satisfactorily from the EEG data without a priori constraints. This gives further support to the conclusion that there is a functional link between BOLD response and slow-wave changes in the EEG.

DISCUSSION

With a paradigm that enforces associative LTM retrieval without confounding recall with perceptual processing, we found evidence for content-specific dynamics of associative LTM retrieval in humans. The RTs of both experiments clearly demonstrated that the time to recall associations from LTM is determined by the number of associations. Correspondingly, the BOLD response and the negative slow-wave maximum increased monotonically with the number of retrieved associations. The locations of this effect dissociated topographically for the two stimulus types, indicating that the activity level of material-specific cortical cell assemblies increased the more associations had to be accessed.

For positions, the strongest parametric activations and the strongest overall activation compared to objects were found in the parietal cortex and precentral gyri, an effect that is mirrored by the EEG, where both the fan effect and the overall slow-wave topography exhibited a pronounced parietal maximum for positions. Thus, all the evidence supports the claim that the parietal lobes as well as the precentral gyri are essential for the retrieval of spatial associations from LTM. The network of activations for objects comprised also the parietal cortex, but here the strongest fan-related activity was found within the left frontal cortex. This finding corresponds again with the EEG data, where recalling objects elicited a pronounced left frontal maximum, as well as with the general fMRI contrast, in which objects, relative to positions, showed a stronger activation in the left middle/inferior frontal gyrus. Therefore, all the evidence suggests that the left middle/inferior frontal gyrus is essentially involved if object associations have to be retrieved from LTM.

The network activated by the fan manipulation bears similarities to a ''frontal–parietal network'' that has been proposed by others for regulating content-unspecific higher cognitive functions, such as mental imagery, working memory control, or LTM retrieval (e.g., Sohn et al., 2005; Mechelli, Price, Friston, & Ishai, 2004; Ishai, Ungerleider, & Haxby, 2000). However, the present data provide clear evidence for a content-*dependent* rather than a content-*independent* involvement of the frontal–parietal network, with a stronger reliance on parietal regions for positions and a stronger reliance on left frontal regions for objects. This was further substantiated by conjunction analyses, which revealed that the right superior parietal lobe showed stronger responses for positions *and* a more pronounced fan effect for positions than for objects, whereas the middle/inferior left frontal gyrus showed the opposite (i.e., a more pronounced fan effect for objects than for positions *and* generally a stronger response for objects than for positions). Furthermore, ANOVAs of the BOLD-signal time courses from these regions showed more activity in the superior parietal lobes during recall of positions than objects and the opposite pattern for the left middle/inferior frontal gyrus. This asymmetric activation can hardly be explained by differences in control processes because the quality and quantity of activated associations was varied systematically while the triggering stimuli, the recall, and the response requirements were held constant. The only difference between objects and positions, which may tentatively be related to material-unspecific control processes, are, on average, the somewhat longer RTs for objects than for positions. However, this difference applies to all fan levels and, therefore, excludes the possibility that the fan-related activation *differences* are due to different levels of retrieval difficulty. Furthermore, in a previous fMRI study (Khader, Burke, Bien, Ranganath, & Rösler, 2005), we had compared the same type of spatial information as used in the present study with a different type of object stimuli (i.e., pictures of faces), and we had found a generally stronger activation and a more pronounced fan effect for object than for position information in the left prefrontal cortex, too. However, in this previous study, the positions had evoked longer retrieval times than faces, whereas in the present study it was exactly the opposite—objects evoked longer retrieval times than positions. Taken together, we conclude that the asymmetry between the prefrontal and parietal cortex, with respect to stimulus type, is not due to unspecific differences in control processes, but rather reflects differences in the activation of content-specific LTM representations.

A somewhat surprising finding of the present study was that we did not observe a fan effect in the hippocampus and related structures of the medial-temporal cortex. According to the neocortical reactivation account of memory representations, the hippocampus serves as a ''trainer'' of the neocortex by repeatedly reactivating those cortical areas in which the stimuli had been perceptually processed (e.g., McClelland et al., 1995; Alvarez & Squire, 1994). A neocortical activation pattern is being initially transmitted to the hippocampus and related mediotemporal structures, forming a compressed image (''address code'') there by means of rapid synaptic changes that allow full reconstruction of the pattern whenever the address code is being activated by external or internal cues (Rolls, 2000; Squire & Alvarez, 1995; Treves & Rolls, 1994; Teyler & DiScenna, 1986). This kind of progressive consolidation is assumed to result in a functional autonomy of the neocortical cell assemblies from the bottleneck structures (Squire & Alvarez, 1995) and remains intact even in patients with complete hippocampectomy (Squire, 1992). Computer simulation models of this process (McClelland et al., 1995; Alvarez & Squire, 1994) are consistent with this notion. They show that repeated training of the neocortex produces an asymptotic state of cortical activation that no longer benefits from hippocampal activations. The present study was explicitly designed to activate highly overlearned information. To ensure that each participant had successfully consolidated the material, we had employed an extensive overlearning procedure before the first retrieval test, and a refreshing overlearning phase before the fMRI recordings took place, ensuring that all participants had full access to all associations. These aspects suggest two explanations for why prominent hippocampal activations were not seen in this study. First, it is possible that retrieval of highly overlearned associations, as realized in our study, is by and large independent from hippocampal support and fully mastered by direct access to cortical representations. Second, the models of neocortical reactivation described above assume that the hippocampus establishes pointers to the neocortical storage sites in which the reactivation proper takes place. Accordingly, the role of the hippocampus is to provide the address codes of the stored representations, and thus, provides only a trigger signal to reactivate the distributed pattern of neocortical LTM representations. This trigger signal will be of similar size during both object and position retrieval because the retrieval situation is completely equivalent for the two conditions. Likewise, it is also conceivable that there are only small differences in hippocampal activations between the three fan conditions because they all involve an activation of cortical ''addresses.''

As noted earlier, material specificity is an essential feature of the distributed model of LTM representations (O'Reilly & Rudy, 2001; McClelland et al., 1995; Squire & Alvarez, 1995). The present study clearly supports this theory by showing that visual objects and visual–spatial positions seem to be represented in anatomically distinct neural subsystems. Importantly, this conclusion follows from an experimental paradigm in which the retrieval of spatial and object associations was clearly separated in time from perceptual processing of those stimuli. Taken together, the results of the present study are compatible with the idea that the dynamics of associative memory retrieval, as reflected by the fan effects (in RTs, BOLD, and slow-wave amplitudes), are common for different materials, whereas the structural bases, as reflected by the different topographies, are clearly content-specific.

Interestingly, in addition to dorsal pathway areas, such as the inferior and superior parietal lobes, the parahippocampal cortex was found to be more active for spatial information retrieval, which supports the notion that this region plays a prominent role in recalling spatial associations (Malkova & Mishkin, 2003; Maguire, Frith, Burgess, Donnett, & O'Keefe, 1998; Parkinson, Murray, & Mishkin, 1988). The parahippocampal cortex receives strong afferent projections from dorsal stream areas (Mishkin, Suzuki, Gadian, & Vargha-Khadem, 1997; Suzuki & Amaral, 1994), and thus, seems to be the major convergence site through which spatial information is transmitted to the hippocampus (Mair, Burk, & Porter, 2003).

In contrast to spatial positions, specific activations for objects were found in the left temporal and frontal cortex. A temporal lobe activation had to be expected for the retrieval of man-made artifacts such as cups, however, considering previous results on associative object memory (e.g., Law et al., 2005; Haxby et al., 2001) and the work on the ventral visual pathway (Mishkin et al., 1983; Ungerleider & Mishkin, 1982), such an activation should have a more ventral maximum (i.e., in the inferior temporal cortex, rather than, as found here, in the middle temporal gyrus). However, retrieving associations from LTM one day or later after their acquisition may comprise a more abstract and elaborate type of semantic knowledge involving a broader set of features that is accessed by the retrieval cues. This argument is supported by studies in which the processing of nouns and semantic knowledge of objects was found to activate the lateral temporal cortex (Damasio, Grabowski, Tranel, Hichwa, & Damasio, 1996), and by lesions of the lateral temporal lobe that impaired both object knowledge and the processing of nouns (Daniele, Giustolini, Silveri, Colosimo, & Gainotti, 1994; Damasio & Tranel, 1993; see Gainotti, 2000, for an overview), and is also consistent with the pronounced left frontal activation for objects often observed during semantic processing (e.g., Binder et al., 1997). In fact, associative memory retrieval of objects elicited the most pronounced activation in the left frontal cortex, which was also found in previous studies of our group using faces as ''object'' stimuli (Khader, Burke, et al., 2005; Khader,

Heil, & Rösler, 2005). In the present study, the set of cups was used in order to avoid verbal labeling of the object exemplars during associative encoding (which occurred to some extent with the face stimuli) because the cups are highly similar to each other (see Figure 1D). Consequently, we had expected that the cups would elicit less verbal associations than faces. This expectation was confirmed by postexperimental debriefings of our participants, who consistently reported that they did not frequently, if at all, use verbal labels to form the object and spatial associations. Nevertheless, the left frontal activation dissociated most reliably between objects and positions, and moreover, although cups and faces most likely evoke verbal labels to a different degree, the left frontal activation was of about the same size as in our previous study. Therefore, we conclude that the left frontal cortex must be involved in the LTM retrieval of objects, and not only if verbal labels are accessed.

A major interpretational advantage of the present paradigm is that all topographic differences found between objects and positions with fMRI and EEG must be attributed to memory retrieval rather than cue processing because the retrieval of object and spatial associations was both triggered by the same type of cue (i.e., words). With this paradigm, it is necessary and inevitable to access stored information by intentionally scanning an associative structure of representations. Otherwise, a correct decision cannot be given in the retrieval task. Moreover, the difficulty of memory scanning was a priori defined, and thus, well controlled by a parametric manipulation.

Convergence of Slow Negative EEG Potentials and fMRI BOLD Responses

The present study provided evidence for a systematic relationship between the BOLD response and brain electrical slow-wave shifts in a highly demanding cognitive task. First, on a phenomenological level, both signals responded similarly to the experimental manipulations. Both methods yielded closely corresponding results with respect to the overall topography of the activation pattern during memory retrieval of different types of information and, most intriguing, both signals reflected the increasing difficulty of the task in a parametric increase of signal strength. This gradual increase also proved to be topographically specific for the two types of material in both experiments. Second, with a model-based approach, it was shown that the relative dipole strengths for positions and objects reflect the relative amount of fMRI activation in the corresponding brain regions when topographical differences of surface-recorded slow waves are modeled with dipoles that are seeded according to the maxima of the BOLD response. Finally, unconstrained estimates of EEG sources showed also substantial overlap with the BOLD activation spots.

Taken together, the correspondence between event-related slow waves and BOLD signals has been proven in the present study by a parallel parametrical activation (''indirect integration''; Luck, 1999) as well as with the similarity of the topographic distributions of both biosignals, which was further substantiated by fMRI-seeded dipole models (''direct integration''). Negative slow waves of the EEG most likely reflect postsynaptic neural activity of cell assemblies that are located underneath or, at least, in close neighborhood of the recording electrode. This claim follows from animal studies (Mitzdorf, 1985, 1991) and biophysical models (Elbert, 1993), and is well supported by the present data that show a clear topographical convergence of the slow wave and the BOLD maxima. Similar congruencies were also reported by Lang et al. (1988), who had measured regional cerebral blood flow and slow waves as well as by Schicke et al. (2006) and Lamm, Windischberger, Leodolter, Moser, and Bauer (2001), who had observed pronounced negative slow waves over those cortical areas that also showed a substantial task-related increase of the hemodynamic response in mental imagery tasks. Moreover, recent evidence from intracranial recordings in monkeys and humans proves of a very close correlation between the BOLD signal and long-lasting local field potentials within the same brain area (Mukamel et al., 2005; Logothetis, Pauls, Augath, Trinath, & Oeltermann, 2001). The present study provides additional evidence that a functional coupling of BOLD signal and neural activity does not only exist in animals during basic sensory stimulation but also in humans during highly demanding cognitive tasks. The close correspondence between the BOLD and EEG responses provides a strong validation of the found fMRI activations by means of a different neuroimaging method applied to the same participants. Furthermore, a joint consideration of all three dependent variables—RTs, EEG slow waves, and BOLD responses—suggests that slow waves conceptually bridge the temporal gap between immediate behavior and the delayed hemodynamic response, and contributes to the formulation of a plausible neurophysiological scenario of how and where material-specific stimulus representations are activated during associative LTM retrieval.

Response times showed that associations must have been retrieved between 3 and 6 sec on average (see Figure 2). The slow-wave fan effects emerged between 2.5 and 6 sec, that is, these effects cover exactly the same temporal window during which, according to the RTs, retrieval activity must have occurred (see Figure 6 and Results). Thus, it seems justified to conclude that the neural activity that becomes manifest in the slow waves is functionally related to the cognitive processes that determine RTs. In contrast, a direct functional link between assumed cognitive processes and the BOLD response is much less evident, as a hemodynamic dissociation of the fan conditions appeared much later, between 5 and

10 sec (i.e., after the retrieval processes have already been completed). However, the close correspondence between locations of significant BOLD responses and seeded generators of the slow waves makes it very likely that both biosignals are driven by activity changes in the very same neural networks, and therefore, the conclusion seems also to be justified that the neural activity reflected by the BOLD effect is functionally linked to behavior and its antecedent cognitive processes. This link is also strongly substantiated by the specific result that the maximum activation developed later in the left frontal dipoles for objects and earlier in the more posterior dipoles for positions (see Figure 8). This temporal difference in dipole strength development corresponds with the original ERPs (see Figure 6A), where the slow-wave fan effect proved significant during later time epochs for objects at left central and frontal electrodes than the fan effect for positions at parietal electrodes. Furthermore, it is consistent with the generally longer RTs and higher error rates for objects, as well as with our participants' subjective reports during debriefing, saying that the object condition was somewhat more difficult than the position condition. This difference is most likely due to the higher visual similarity of the cups than the spatial positions.

One may argue that a convincing integration of EEG and fMRI results is questionable in the present study because the participants were tested twice with a substantial delay between the two testing sessions, and therefore, the two measurement situations might not be equivalent with respect to the triggered retrieval processes. However, there are several arguments in favor of the conclusion that fully consolidated representations were activated in both sessions and that the very same retrieval processes were invoked. As outlined, the present study was designed to activate fully consolidated information from LTM. To ensure this, an extensive overlearning procedure was administered before the first retrieval test and a refreshing overlearning phase was completed before the fMRI recording (see Methods section). Thus, before each measurement (EEG and fMRI), each participant was tested on the same high-performance level (i.e., at the end of overlearning, each participant committed less than 5% of retrieval errors). This is an extremely small rate of errors, considering the complexity of the material and the time needed to achieve this performance level. The initial overlearning phase took about 1–2 hours. The second, refreshing overlearning session, before the fMRI measurement, took about 15–30 min only, which clearly shows that it comprised only an updating of already well-established memory traces. Moreover, RTs and error rates were affected by the experimental variables (type of material, level of fan) equivalently in both sessions.[1] This congruency of the complete pattern of behavioral data is direct empirical evidence for the conclusion that the same cognitive processes must have been triggered. Finally, in a previous set of studies, our group has shown that reliable and equivalent modulations of the BOLD effect are evoked in the fan retrieval paradigm regardless of whether the participants were tested in the scanner one day after learning without an intervening EEG retrieval phase and without a fresh-up procedure prior to scanning or, as in the present study, after a delay of several days and a refreshing procedure (Khader, Burke, et al., 2005).

Conclusions

Based on the parallel parametric activations and topographies, together with the fMRI-seeded dipole models, we propose that associative LTM representations are stored and reactivated in distributed and content-specific cortical cell assemblies. These neural networks are widely distributed and comprise both anterior and posterior cortex areas. They show substantial overlap for distinct contents, but they have, nevertheless, a content-specific topography that partially overlaps with sensory cortices specialized for the perceptual processing of equivalent stimulus features. Further studies must disclose the functional differentiation of the local and anatomically distinct circuits that form the elements of these large-scale networks. In the present study, both anterior and posterior areas reflected material-specific and load-related activation patterns. Therefore, one has to conclude that anterior ''control'' and posterior ''buffer'' areas both embody content-specific circuits and that both are also actively involved during memory retrieval. The observed activation patterns are compatible with the idea that learned associations are retrieved from LTM by an interactive ''cross-talk'' between all subcircuits of the content-specific large-scale networks, and that this cross-talk takes longer and becomes more effortful for all involved cell assemblies the more associations have to be reactivated.

Acknowledgments

This work was supported by Grant FOR254/2 of the German Research Foundation (DFG) assigned to F. R. We thank Martin Heil and Erwin Hennighausen for assistance, and Kerstin Jost and Linda Muray for valuable discussions and helpful comments on the manuscript.

Reprint requests should be sent to Patrick Khader, Department of Psychology, Philipps-University, 35032 Marburg, Germany, or via e-mail: Khader@staff.uni-marburg.de, URL: http://staff-www.uni-marburg.de/~cablab.

Note

1. In order to test whether the pattern of results was essentially the same for the EEG and fMRI phases of the experiment, we compared both datasets directly in an ANOVA with factors fan level, material type, and dataset (EEG, fMRI). These analyses did not reveal any significant main effect of dataset or

interaction between factor dataset and material type or fan level (all $p > .05$), neither for the RTs nor for the error rates.

REFERENCES

Alvarez, P., & Squire, L. R. (1994). Memory consolidation and the medial temporal lobe: A simple network model. *Proceedings of the National Academy of Sciences, U.S.A., 91,* 7041–7045.

Anderson, J. R. (1974). Retrieval of propositional information from long-term memory. *Cognitive Psychology, 6,* 451–474.

Anderson, J. R., & Bower, G. H. (1973). *Human associative memory.* Washington, DC: Winston & Sons.

Binder, J. R., Frost, J. A., Hammeke, T. A., Cox, R. W., Rao, S. M., & Prieto, T. (1997). Human brain language areas identified by functional magnetic resonance imaging. *Journal of Neuroscience, 17,* 353–362.

Buckner, R. L., & Wheeler, M. E. (2001). The cognitive neuroscience of remembering. *Nature Reviews Neuroscience, 2,* 624–634.

Christoff, K., Prabhakaran, V., Dorfman, J., Zhao, Z., Kroger, J. K., Holyoak, K. J., et al. (2001). Rostrolateral prefrontal cortex involvement in relational integration during reasoning. *Neuroimage, 14,* 1136–1149.

Damasio, A. R., & Tranel, D. (1993). Nouns and verbs are retrieved with differently distributed neural systems. *Proceedings of the National Academy of Sciences, U.S.A., 90,* 457–460.

Damasio, H., Grabowski, T. J., Tranel, D., Hichwa, R. D., & Damasio, A. R. (1996). A neural basis for lexical retrieval. *Nature, 380,* 499–505.

Daniele, A., Giustolini, M., Silveri, M., Colosimo, C., & Gainotti, G. (1994). Evidence for a possible neuroanatomical basis for lexical processing of nouns and verbs. *Neuropsychologia, 32,* 1325–1341.

Deese, J. (1965). *The structure of associations in language and thought.* Baltimore: John Hopkins Press.

Elbert, T. (1993). Slow cortical potentials reflect the regulation of cortical excitability. In W. C. McCallum & C. S. Hutch (Eds.), *Slow potential changes in the human brain* (pp. 235–251). New York: Plenum.

Fujimichi, R., Naya, Y., & Miyashita, Y. (2004). Associative memory: Representation, activation, and cognitive control. In M. S. Gazzaniga (Ed.), *The cognitive neurosciences* (3rd ed., pp. 905–918). Cambridge: MIT Press.

Gainotti, G. (2000). What the locus of brain lesion tells us about the nature of the cognitive defect underlying category-specific disorders: A review. *Cortex, 36,* 539–559.

Haxby, J. V., Gobbini, M. I., Furey, M. L., Ishai, A., Schouten, J. L., & Pietrini, P. (2001). Distributed and overlapping representations of faces and objects in ventral temporal cortex. *Science, 293,* 2425–2430.

Heil, M., Rösler, F., & Hennighausen, E. (1994). Dynamics of activation in long-term memory: The retrieval of verbal, pictorial, spatial, and color information. *Journal of Experimental Psychology: Learning, Memory, and Cognition, 20,* 185–200.

Hennighausen, E., Heil, M., & Rösler, F. (1993). A correction method for DC drift artifacts. *Electroencephalography and Clinical Neurophysiology, 86,* 199–204.

Huynh, H., & Feldt, L. S. (1970). Conditions under which mean square ratios repeated measurements designs have exact F-distributions. *Journal of the American Statistical Association, 65,* 1582–1589.

Ishai, A., Ungerleider, L. G., & Haxby, J. V. (2000). Distributed neural systems for the generation of visual images. *Neuron, 28,* 979–990.

Khader, P., Burke, M., Bien, S., Ranganath, C., & Rösler, F. (2005). Content-specific activation during associative long-term memory retrieval. *Neuroimage, 27,* 805–816.

Khader, P., Heil, M., & Rösler, F. (2005). Material-specific long-term memory representations of faces and spatial positions: Evidence from slow event-related brain potentials. *Neuropsychologia, 43,* 2109–2124.

Kriegeskorte, N., & Göbel, R. (2001). An efficient algorithm for topologically correct segmentation of the cortical sheet in anatomical MR volumes. *Neuroimage, 14,* 329–346.

Lamm, C., Windischberger, C., Leodolter, U., Moser, E., & Bauer, H. (2001). Evidence for premotor cortex activity during dynamic visuospatial imagery from single-trial functional magnetic resonance imaging and event-related slow cortical potentials. *Neuroimage, 14,* 268–283.

Lang, W., Lang, M., Podreka, I., Steiner, M., Uhl, F., Suess, E., et al. (1988). DC-potential shifts and regional cerebral blood flow reveal frontal cortex involvement in human visuomotor learning. *Experimental Brain Research, 71,* 353–364.

Law, J. R., Flanery, M. A., Wirth, S., Yanike, M., Smith, A. C., Frank, L. M., et al. (2005). Functional magnetic resonance imaging activity during the gradual acquisition and expression of paired-associative memory. *Journal of Neuroscience, 25,* 5720–5729.

Logothetis, N. K., Pauls, J., Augath, M., Trinath, T., & Oeltermann, A. (2001). Neurophysiological investigation of the basis of the fMRI signal. *Nature, 412,* 150–157.

Luck, S. J. (1999). Direct and indirect integration of event-related potentials, functional magnetic resonance images, and single-unit recordings. *Human Brain Mapping, 8,* 115–201.

Maguire, E. A., Frith, C. D., Burgess, N., Donnett, J. G., & O'Keefe, J. (1998). Knowing where things are: Parahippocampal involvement in encoding object locations in virtual large-scale space. *Journal of Cognitive Neuroscience, 10,* 61–76.

Mair, R. G., Burk, J. A., & Porter, M. C. (2003). Impairment of radial maze delayed nonmatching after lesions of anterior thalamus and parahippocampal cortex. *Behavioral Neuroscience, 117,* 596–605.

Malkova, L., & Mishkin, M. (2003). One-trial memory for object-place associations after separate lesions of hippocampus and posterior parahippocampal region in the monkey. *Journal of Neuroscience, 23,* 1956–1965.

Masson, M. E. J. (1995). A distributed memory model of semantic priming. *Journal of Experimental Psychology: Learning, Memory, and Cognition, 21,* 3–23.

McCallum, W. C., & Curry, S. H. (Eds.) (1993). *Slow potential changes in the human brain.* New York: Plenum.

McClelland, J. L., McNaughton, B. L., & O'Reilly, R. C. (1995). Why there are complementary learning systems in the hippocampus and neocortex: Insights from the successes and failures of connectionist models of learning and memory. *Psychological Review, 102,* 419–457.

Mechelli, A., Price, C. J., Friston, K. J., & Ishai, A. (2004). Where bottom-up meets top-down: Neuronal interactions during perception and imagery. *Cerebral Cortex, 14,* 1256–1265.

Mishkin, M., Suzuki, W. A., Gadian, D. G., & Vargha-Khadem, F. (1997). Hierarchical organization of cognitive memory. *Philosophical Transactions of the Royal Society of London, Series B, Biological Sciences, 352,* 1461–1467.

Mishkin, M., Ungerleider, L. G., & Macko, K. A. (1983). Object vision and spatial vision: Two cortical pathways. *Trends in Neurosciences, 6,* 414–417.

Mitzdorf, U. (1985). Current source-density method and application in cat cerebral cortex: Investigation of evoked

potentials and EEG phenomena. *Physiological Reviews, 65,* 37–100.
Mitzdorf, U. (1991). Physiological sources of evoked potentials. C. H. M. Brunia, G. Mulder, & M. N. Verbaten (Eds.), *Event-related brain research* (pp. 47–57). Amsterdam: Elsevier.
Miyashita, Y. (1988). Neuronal correlates of visual associative long-term memory in the primate temporal cortex. *Nature, 335,* 817–820.
Miyashita, Y., Kameyama, M., Hasegawa, I., & Fukushima, T. (1998). Consolidation of visual associative long-term memory in the temporal cortex of primates. *Neurobiology of Learning and Memory, 70,* 197–211.
Mukamel, R., Gelbard, H., Arieli, A., Hasson, U., Fried, I., & Malach, R. (2005). Coupling between neuronal firing, field potentials, and fMRI in human auditory cortex. *Science, 309,* 951–954.
Naya, Y., Yoshida, M., & Miyashita, Y. (2001). Backward spreading of memory-retrieval signal in the primate temporal cortex. *Science, 291,* 661–664.
Nyberg, L., Habib, R., McIntosh, A. R., & Tulving, E. (2000). Reactivation of encoding-related brain activity during memory retrieval. *Proceedings of the National Academy of Sciences, U.S.A., 97,* 11120–11124.
Nyberg, L., Persson, K. M., Nilsson, L. G., Sandblom, J., Aberg, C., & Ingvar, M. (2001). Reactivation of motor brain areas during explicit memory for actions. *Neuroimage, 14,* 521–528.
O'Reilly, R. C., & Rudy, J. W. (2001). Conjunctive representations in learning and memory: Principles of cortical and hippocampal function. *Psychological Review, 108,* 311–345.
Parkinson, J. K., Murray, E. A., & Mishkin, M. (1988). A selective mnemonic role for the hippocampus in monkeys: Memory for the location of objects. *Journal of Neuroscience, 8,* 4159–4167.
Ranganath, C., & D'Esposito, M. (2001). Medial temporal lobe activity associated with active maintenance of novel information. *Neuron, 31,* 865–873.
Rolls, E. T. (2000). Memory systems in the brain. *Annual Review of Psychology, 51,* 599–630.
Rösler, F., Heil, M., & Hennighausen, E. (1995). Distinct cortical activation patterns during long-term memory retrieval of verbal, spatial and color information. *Journal of Cognitive Neuroscience, 7,* 51–65.
Rösler, F., Heil, M., & Röder, B. (1997). Slow negative brain potentials as reflections of specific modular resources of cognition. *Biological Psychology, 45,* 109–141.
Rugg, M. D., & Wilding, E. L. (2000). Retrieval processing and episodic memory. *Trends in Cognitive Sciences, 4,* 108–115.
Sakai, K., & Miyashita, Y. (1991). Neural organization for the long-term memory of paired associates. *Nature, 354,* 152–155.
Schicke, T., Muckli, L., Beer, A. L., Wibral, M., Singer, W., Goebel, R., et al. (2006). Tight covariation of BOLD signal changes and slow ERPs in the parietal cortex in a parametric spatial imagery task with haptic acquisition. *European Journal of Neuroscience, 23,* 1910–1918.
Sohn, M. H., Goode, A., Stenger, V. A., Carter, C. S., & Anderson, J. R. (2003). Competition and representation during memory retrieval: Roles of the prefrontal cortex and the posterior parietal cortex. *Proceedings of the National Academy of Sciences, U.S.A., 100,* 7412–7417.
Sohn, M. H., Goode, A., Stenger, V. A., Jung, K. J., Carter, C. S., & Anderson, J. R. (2005). An information-processing model of three cortical regions: Evidence in episodic memory retrieval. *Neuroimage, 25,* 21–33.
Speckmann, E. J., Caspers, H., & Elger, C. (1984). Neuronal mechanisms underlying the generation of field potentials. In T. Elbert, B. Rockstroh, W. Lutzenberger, & N. Birbaumer (Eds.), *Self-regulation of the brain and behavior* (pp. 9–25). Heidelberg: Springer.
Squire, L. R. (1992). Memory and the hippocampus: A synthesis from findings with rats, monkeys, and humans. *Psychological Review, 99,* 195–231.
Squire, L. R., & Alvarez, P. (1995). Retrograde amnesia and memory consolidation: A neurobiological perspective. *Current Opinion in Neurobiology, 5,* 169–177.
Suzuki, W. A., & Amaral, D. G. (1994). Perirhinal and parahippocampal cortices of the macaque monkey: Cortical afferents. *Journal of Comparative Neurology, 350,* 497–533.
Talairach, J., & Tournoux, P. (1988). *Co-planar sterotaxic atlas of the human brain.* Stuttgart: Thieme.
Teyler, T. J., & DiScenna, P. (1986). The hippocampal memory indexing theory. *Behavioral Neuroscience, 100,* 147–154.
Treves, A., & Rolls, E. T. (1994). Computational analysis of the role of the hippocampus in memory. *Hippocampus, 4,* 374–391.
Ungerleider, L. G., & Mishkin, M. (1982). Two cortical visual systems. In D. J. Ingle, M. A. Goodale, & R. J. Mansfield (Eds.), *Analysis of visual behavior* (pp. 549–580). Cambridge: MIT Press.
Wheeler, M. E., & Buckner, R. L. (2003). Functional dissociation among components of remembering: Control, perceived oldness, and content. *Journal of Neuroscience, 23,* 3869–3880.
Wheeler, M. E., Petersen, S. E., & Buckner, R. L. (2000). Memory's echo: Vivid remembering reactivates sensory-specific cortex. *Proceedings of the National Academy of Sciences, U.S.A., 97,* 11125–11129.
Wirth, S., Yanike, M., Smith, A., Brown, E., & Suzuki, W. (2003). Single neurons in the monkey hippocampus and learning of new associations. *Science, 300,* 1578–1581.

This article has been cited by:

1. Paul Metzner, Titus von der Malsburg, Shravan Vasishth, Frank Rösler. 2017. The Importance of Reading Naturally: Evidence From Combined Recordings of Eye Movements and Electric Brain Potentials. *Cognitive Science* **41**, 1232-1263. [Crossref]
2. Jelmer P. Borst, Avniel S. Ghuman, John R. Anderson. 2016. Tracking cognitive processing stages with MEG: A spatio-temporal model of associative recognition in the brain. *NeuroImage* **141**, 416-430. [Crossref]
3. Patrick H. Khader, Thorsten Pachur, Lilian A. E. Weber, Kerstin Jost. 2016. Neural Signatures of Controlled and Automatic Retrieval Processes in Memory-based Decision-making. *Journal of Cognitive Neuroscience* **28**:1, 69-83. [Abstract] [Full Text] [PDF] [PDF Plus]
4. Katarina Forkmann, Katja Wiech, Tobias Sommer, Ulrike Bingel. 2015. Reinstatement of pain-related brain activation during the recognition of neutral images previously paired with nociceptive stimuli. *PAIN* **156**:8, 1501-1510. [Crossref]
5. Jelmer P. Borst, John R. Anderson. 2015. The discovery of processing stages: Analyzing EEG data with hidden semi-Markov models. *NeuroImage* **108**, 60-73. [Crossref]
6. Jelmer P. Borst, Darryl W. Schneider, Matthew M. Walsh, John R. Anderson. 2013. Stages of Processing in Associative Recognition: Evidence from Behavior, EEG, and Classification. *Journal of Cognitive Neuroscience* **25**:12, 2151-2166. [Abstract] [Full Text] [PDF] [PDF Plus]
7. Marieke L. Schölvinck, David A. Leopold, Matthew J. Brookes, Patrick H. Khader. 2013. The contribution of electrophysiology to functional connectivity mapping. *NeuroImage* **80**, 297-306. [Crossref]
8. Zara M. Bergström, Richard N. Henson, Jason R. Taylor, Jon S. Simons. 2013. Multimodal imaging reveals the spatiotemporal dynamics of recollection. *NeuroImage* **68**, 141-153. [Crossref]
9. J. Matias Palva, Satu Palva. 2012. Infra-slow fluctuations in electrophysiological recordings, blood-oxygenation-level-dependent signals, and psychophysical time series. *NeuroImage* **62**:4, 2201-2211. [Crossref]
10. Maria Wimber, Anne Maaß, Tobias Staudigl, Alan Richardson-Klavehn, Simon Hanslmayr. 2012. Rapid Memory Reactivation Revealed by Oscillatory Entrainment. *Current Biology* **22**:16, 1482-1486. [Crossref]
11. Kerstin Jost, Patrick H. Khader, Peter Düsel, Franziska R. Richter, Kristina B. Rohde, Siegfried Bien, Frank Rösler. 2012. Controlling Conflict from Interfering Long-term Memory Representations. *Journal of Cognitive Neuroscience* **24**:5, 1173-1190. [Abstract] [Full Text] [PDF] [PDF Plus]
12. Zara M. Bergström, Richard J. O'Connor, Martin K.-H. Li, Jon S. Simons. 2012. Event-related potential evidence for separable automatic and controlled retrieval processes in proactive interference. *Brain Research* **1455**, 90-102. [Crossref]
13. J.M. Kızılırmak, F. Rösler, P.H. Khader. 2012. Control processes during selective long-term memory retrieval. *NeuroImage* **59**:2, 1830-1841. [Crossref]
14. Patrick H. Khader, Thorsten Pachur, Stefanie Meier, Siegfried Bien, Kerstin Jost, Frank Rösler. 2011. Memory-based Decision-making with Heuristics: Evidence for a Controlled Activation of Memory Representations. *Journal of Cognitive Neuroscience* **23**:11, 3540-3554. [Abstract] [Full Text] [PDF] [PDF Plus]
15. Jared F. Danker, Jon M. Fincham, John R. Anderson. 2011. The neural correlates of competition during memory retrieval are modulated by attention to the cues. *Neuropsychologia* **49**:9, 2427-2438. [Crossref]
16. Rolf Verleger, Janna Ludwig, Vasil Kolev, Juliana Yordanova, Ullrich Wagner. 2011. Sleep effects on slow-brain-potential reflections of associative learning. *Biological Psychology* **86**:3, 219-229. [Crossref]
17. Patrick H. Khader, Frank Rösler. 2011. EEG power changes reflect distinct mechanisms during long-term memory retrieval. *Psychophysiology* **48**:3, 362-369. [Crossref]
18. Hubert D. Zimmer, Ullrich K.H. Ecker. 2010. Remembering perceptual features unequally bound in object and episodic tokens: Neural mechanisms and their electrophysiological correlates. *Neuroscience & Biobehavioral Reviews* **34**:7, 1066-1079. [Crossref]
19. Ulrike Malecki, Sabine Stallforth, Dorothee Heipertz, Nilli Lavie, Emrah Duzel. 2009. Neural generators of sustained activity differ for stimulus-encoding and delay maintenance. *European Journal of Neuroscience* **30**:5, 924-933. [Crossref]
20. Juliana Yordanova, Vasil Kolev, Ullrich Wagner, Rolf Verleger. 2009. Covert Reorganization of Implicit Task Representations by Slow Wave Sleep. *PLoS ONE* **4**:5, e5675. [Crossref]
21. Oliver Stock, Brigitte Röder, Michael Burke, Siegfried Bien, Frank Rösler. 2009. Cortical Activation Patterns during Long-term Memory Retrieval of Visually or Haptically Encoded Objects and Locations. *Journal of Cognitive Neuroscience* **21**:1, 58-82. [Abstract] [Full Text] [PDF] [PDF Plus]
22. Patrick Khader, Tobias Schicke, Brigitte Röder, Frank Rösler. 2008. On the relationship between slow cortical potentials and BOLD signal changes in humans. *International Journal of Psychophysiology* **67**:3, 252-261. [Crossref]